Simultaneous SNP selection and adjustment for population structure in high dimensional prediction models

Sahir R Bhatnagar[1,2], Karim Oualkacha[3], Yi Yang[4], Tianyuan Lu[2], Marie Forest[2], and Celia MT Greenwood[1,2,5]

[1]Department of Epidemiology, Biostatistics and Occupational Health, McGill University

[2]Lady Davis Institute, Jewish General Hospital, Montréal, QC

[3]Département de Mathématiques, Université de Québec À Montréal

[4]Department of Mathematics and Statistics, McGill University

[5]Departments of Oncology and Human Genetics, McGill University

June 13, 2019

Abstract

Complex traits are known to be influenced by a combination of environmental factors and rare and common genetic variants. However, detection of such multivariate associations can be compromised by low statistical power and confounding by population structure. Linear mixed effect models (LMM) can account for correlations due to relatedness but have not been applicable in high-dimensional (HD) settings where

1

the number of fixed effect predictors greatly exceeds the number of samples. False positives can result from two-stage approaches, where the residuals estimated from a null model adjusted for the subjects' relationship structure are subsequently used as the response in a standard penalized regression model. To overcome these challenges, we develop a general penalized LMM framework called `ggmix` that simultaneously, in one step, selects SNPs and estimates their effects, while adjusting for population structure. Our method can accommodate several sparsity-inducing penalties such as the lasso, elastic net and group lasso, and also readily handles prior annotation information in the form of weights. We develop a blockwise coordinate descent algorithm which is highly scalable, computationally efficient and has theoretical guarantees of convergence. Through simulations, we show that `ggmix` leads to correct Type 1 error control and improved variance component estimation compared to the two-stage approach or principal component adjustment. `ggmix` is also robust to different kinship structures and heritability proportions. Our algorithms are available in an R package (https://github.com/greenwoodlab).

1   Author Summary

2   Introduction

Genome-wide association studies (GWAS) have become the standard method for analyzing genetic datasets owing to their success in identifying thousands of genetic variants associated with complex diseases (https://www.genome.gov/gwastudies/). Despite these impressive findings, the discovered markers have only been able to explain a small proportion of the phenotypic variance; this is known as the missing heritability problem [1]. One plausible explanation is that there are many causal variants that each explain a small amount of variation with small effect sizes [2]. Methods such GWAS, which test each variant or single

nucleotide polymorphism (SNP) independently, may miss these true associations due to the stringent significance thresholds required to reduce the number of false positives [1]. Another major issue to overcome is that of confounding due to geographic population structure, family and/or cryptic relatedness which can lead to spurious associations [3]. For example, there may be subpopulations within a study that differ with respect to their genotype frequencies at a particular locus due to geographical location or their ancestry. This heterogeneity in genotype frequency can cause correlations with other loci and consequently mimic the signal of association even though there is no biological association [4, 5]. Studies that separate their sample by ethnicity to address this confounding suffer from a loss in statistical power.

To address the first problem, multivariable regression methods have been proposed which simultaneously fit many SNPs in a single model [6, 7]. Indeed, the power to detect an association for a given SNP may be increased when other causal SNPs have been accounted for. Conversely, a stronger signal from a causal SNP may weaken false signals when modeled jointly [6].

Solutions for confounding by population structure have also received significant attention in the literature [8, 9, 10, 11]. There are two main approaches to account for the relatedness between subjects: 1) the principal component (PC) adjustment method and 2) the linear mixed model (LMM). The PC adjustment method includes the top PCs of genome-wide SNP genotypes as additional covariates in the model [12]. The LMM uses an estimated covariance matrix from the individuals' genotypes and includes this information in the form of a random effect [3].

While these problems have been addressed in isolation, there has been relatively little progress towards addressing them jointly at a large scale. Region-based tests of association have been developed where a linear combination of p variants is regressed on the response variable in a mixed model framework [13]. In case-control data, a stepwise logistic-regression procedure was used to evaluate the relative importance of variants within a small genetic

⁶⁹ region [14]. These methods however are not applicable in the high-dimensional setting, i.e.,

⁷⁰ when the number of variables p is much larger than the sample size n, as is often the case in

⁷¹ genetic studies where millions of variants are measured on thousands of individuals.

⁷² There has been recent interest in using penalized linear mixed models, which place a con-

⁷³ straint on the magnitude of the effect sizes while controlling for confounding factors such as

⁷⁴ population structure. For example, the LMM-lasso [15] places a Laplace prior on all main

⁷⁵ effects while the adaptive mixed lasso [16] uses the L_1 penalty [17] with adaptively chosen

⁷⁶ weights [18] to allow for differential shrinkage amongst the variables in the model. Another

⁷⁷ method applied a combination of both the lasso and group lasso penalties in order to select

⁷⁸ variants within a gene most associated with the response [19]. However, these methods are

⁷⁹ normally performed in two steps. First, the variance components are estimated once from

⁸⁰ a LMM with a single random effect. These LMMs normally use the estimated covariance

⁸¹ matrix from the individuals' genotypes to account for the relatedness but assumes no SNP

⁸² main effects (i.e. a null model). The residuals from this null model with a single random

⁸³ effect can be treated as independent observations because the relatedness has been effec-

⁸⁴ tively removed from the original response. In the second step, these residuals are used as the

⁸⁵ response in any high-dimensional model that assumes uncorrelated errors. This approach

⁸⁶ has both computational and practical advantages since existing penalized regression soft-

⁸⁷ ware such as `glmnet` [20] and `gglasso` [21], which assume independent observations, can be

⁸⁸ applied directly to the residuals. However, recent work has shown that there can be a loss in

⁸⁹ power if a causal variant is included in the calculation of the covariance matrix as its effect

⁹⁰ will have been removed in the first step [13, 22].

⁹¹ In this paper we develop a general penalized LMM framework called `ggmix` that simul-

⁹² taneously selects variables and estimates their effects, accounting for between-individual

⁹³ correlations. Our method can accommodate several sparsity inducing penalties such as the

⁹⁴ lasso [17], elastic net [23] and group lasso [24]. `ggmix` also readily handles prior annota-

tion information in the form of a penalty factor, which can be useful, for example, when dealing with rare variants. We develop a blockwise coordinate descent algorithm which is highly scalable and has theoretical guarantees of convergence to a stationary point. All of our algorithms are implemented in the `ggmix` R package hosted on GitHub with extensive documentation (http://sahirbhatnagar.com/ggmix/). We provide a brief demonstration of the `ggmix` package in Appendix C.

The rest of the paper is organized as follows. Section 2 describes the `ggmix` model. Section 3 contains the optimization procedure and the algorithm used to fit the `ggmix` model. In Section 4, we compare the performance of our proposed approach and demonstrate the scenarios where it can be advantageous to use over existing methods through simulation studies. Section 5 discusses some limitations and future directions.

3   Results

In this section we demonstrate the performance of `ggmix` in a simulation study and two real data applications.

3.1   Simulation Study

We evaluated the performance of `ggmix` in a variety of simulated scenarios. For each simulation scenario we compared `ggmix` to the lasso and the twostep method. For the lasso, we included the top 10 principal components from the simulated genotypes used to calculate the kinship matrix as unpenalized predictors in the design matrix. For the twostep method, we first fitted an intercept only model with a single random effect using the average information restricted maximum likelihood (AIREML) algorithm [25] as implemented in the `gaston` R package [26]. The residuals from this model were then used as the response in a regular lasso model. Note that in the twostep method, we removed the kinship effect in the first

118 step and therefore did not need to make any further adjustments when fitting the penalized

119 model. We fitted the lasso using the default settings in the `glmnet` package [20]. For other

120 parameters in our simulation study, we defined the following quantities:

121 • n: sample size

122 • c: percentage of causal SNPs

123 • $\boldsymbol{\beta}$: true effect size vector of length p_{fixed}

124 • $S_0 = \{j; (\boldsymbol{\beta})_j \neq 0\}$ the index of the true active set with cardinality $|S_0| = c \times p_{fixed}$

125 • $\mathbf{X}^{(fixed)}$: $n \times p_{fixed}$ matrix of SNPs that were included as fixed effects in the model

126 • $\mathbf{X}^{(causal)}$: $n \times |S_0|$ matrix of SNPs that were truly associated with the simulated phe-

127   notype, where $\mathbf{X}^{(causal)} \subseteq \mathbf{X}^{(fixed)}$

128 • $\mathbf{X}^{(other)}$: $n \times p_{other}$ matrix of SNPs that were used in the construction of the kinship

129   matrix. Some of these $\mathbf{X}^{(other)}$ SNPs, in conjunction with some of the SNPs in $\mathbf{X}^{(fixed)}$

130   were used in construction of the kinship matrix. We altered the balance between these

131   two contributors and with the proportion of causal SNPs used to calculate kinship

132 • $\mathbf{X}^{(kinship)}$: $n \times k$ matrix of SNPs used to construct the kinship matrix

133 We simulated data from the model

$$\mathbf{Y} = \mathbf{X}^{(fixed)}\boldsymbol{\beta} + \mathbf{P} + \boldsymbol{\varepsilon} \tag{1}$$

134 where $\mathbf{P} \sim \mathcal{N}(0, \eta\sigma^2\boldsymbol{\Phi})$ is the polygenic effect and $\boldsymbol{\varepsilon} \sim \mathcal{N}(0, (1-\eta)\sigma^2\mathbf{I})$ is the error term.

135 Here, $\boldsymbol{\Phi}_{n \times n}$ is the covariance matrix calculated from $\mathbf{X}^{(kinship)}$, $\mathbf{I}_{n \times n}$ is the identity matrix

136 and parameters σ^2 and $\eta \in [0, 1]$ determine how the variance is divided between $\mathbf{P}$ and

137 $\boldsymbol{\varepsilon}$. The values of the parameters that we used were as follows: narrow sense heritability

138 $\eta = \{0.1, 0.5\}$, number of fixed effects $p_{fixed} = 5000$, number of SNPs used to calculate the

139 kinship matrix $k = 10000$, percentage of causal SNPs $c = \{0\%, 1\%\}$ and $\sigma^2 = 1$. In addition

to these parameters, we also varied the amount of overlap between the causal SNPs and the SNPs used to generate the kinship matrix. We considered two main scenarios:

1. None of the causal SNPs are included in the calculation of the kinship matrix:

$$\mathbf{X}^{(kinship)} = \left[\mathbf{X}^{(other)} \right]$$

2. All the causal SNPs are included in the calculation of the kinship matrix:

$$\mathbf{X}^{(kinship)} = \left[\mathbf{X}^{(other)}; \mathbf{X}^{(causal)} \right].$$

Both kinship matrices were meant to contrast the model behavior when the causal SNPs are included in both the main effects and random effects versus when the causal SNPs are only included in the main effects. These scenarios are motivated by the current standard of practice in GWAS where the candidate marker is excluded from the calculation of the kinship matrix [8]. This approach becomes much more difficult to apply in large-scale multivariable models where there is likely to be overlap between the variables in the design matrix and kinship matrix. We simulated random genotypes from the BN-PSD admixture model with 1D geography and 3 subpopulations using the `bnpsd` package [27, 28]. In Figure **??**, we plot the estimated kinship matrix from a single simulated dataset in the form of a heatmap where a darker color indicates a closer genetic relationship.

In Figure **??** we plot the first two principal component scores calculated from the simulated genotypes used to calculate the kinship matrix in Figure **??**, and color each point by sub-population membership. We can see that the PCs can identify the subpopulations which is why including them as additional covariates in a regression model has been considered a reasonable approach to control for confounding.

Using this set-up, we randomly partitioned 2000 simulated observations into 60% for train-

ing, 20% for model selection and 20% for testing. The training set was used to fit the model, the model selection set was used to select the optimal tuning parameter only, and the resulting model was evaluated on the test set. Let $\hat{\lambda}$ be the estimated value of the optimal regularization parameter, $\widehat{\boldsymbol{\beta}}_{\hat{\lambda}}$ the estimate of $\boldsymbol{\beta}$ at regularization parameter $\hat{\lambda}$, and $\widehat{S}_{\hat{\lambda}} = \left\{ j; (\widehat{\boldsymbol{\beta}}_{\hat{\lambda}})_j \neq 0 \right\}$ the index of the set of non-zero estimated coefficients. We evaluated the methods based on correct sparsity defined as $\frac{1}{p} \sum_{j=1}^{p} A_j$, where

$$
A_j = \begin{cases} 1 & \text{if } (\widehat{\boldsymbol{\beta}}_{\hat{\lambda}})_j = (\boldsymbol{\beta})_j = 0 \\ 1 & \text{if } (\widehat{\boldsymbol{\beta}}_{\hat{\lambda}})_j \neq 0, (\boldsymbol{\beta})_j \neq 0 \\ 0 & \text{if else.} \end{cases}
$$

We also compared the test set prediction error, true positive rate $(|\widehat{S}_{\hat{\lambda}} \in S_0|/|S_0|)$, false positive rate $(|\widehat{S}_{\hat{\lambda}} \notin S_0|/|j \notin S_0|)$, and the variance components (η, σ^2) for the polygenic random effect and error term.

Here we present the results for the model with 1% causal SNPs $(c = 0.01)$, and results for the null model $(c = 0)$ in supplementary Section B. In Figure 1 we see that ggmixoutperforms both the twostep and lasso in terms of correct sparsity regardless of true heritability and whether the causal SNPs were included in the calculation of the kinship matrix.

The true positive vs. false positive rate for the model with 1% causal SNPs $(c = 0.01)$ is shown in Figure 3. Both the lasso and twostep outperform ggmix in terms of identifying the true model. This accuracy however, comes at the cost of a very high false positive rate compared to ggmix.

Correct Sparsity results for the Model with 1% Causal SNPs
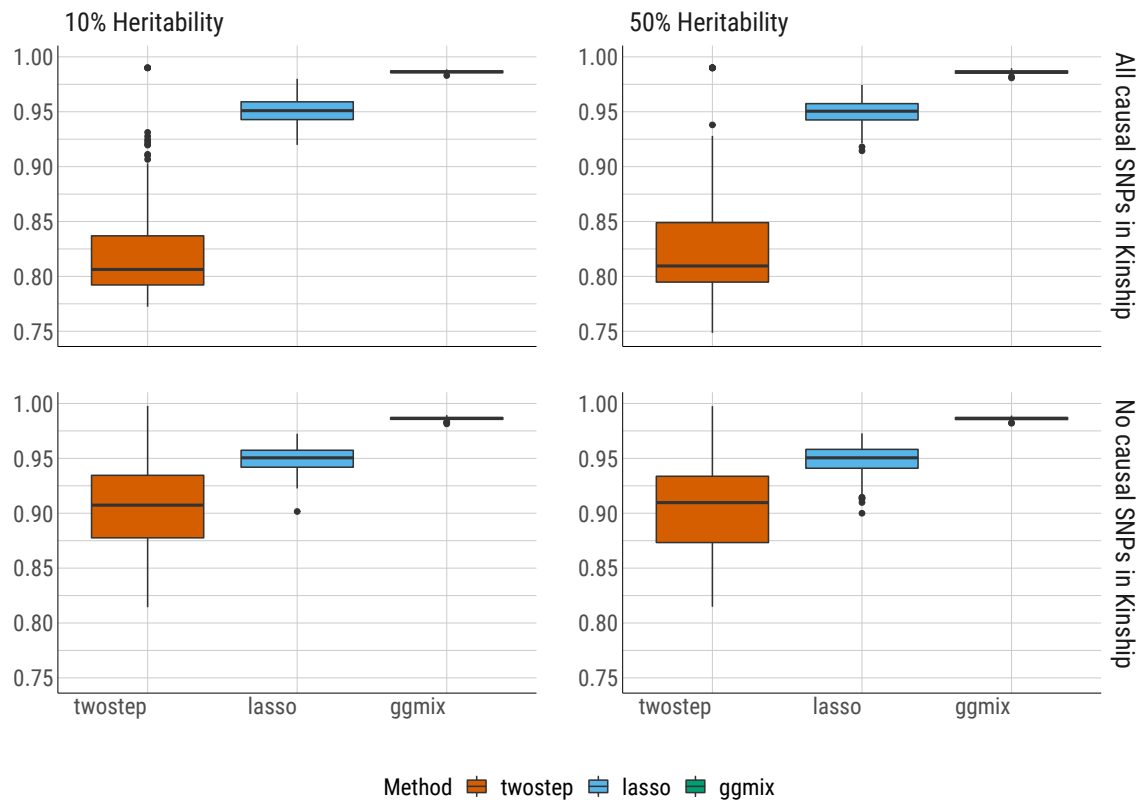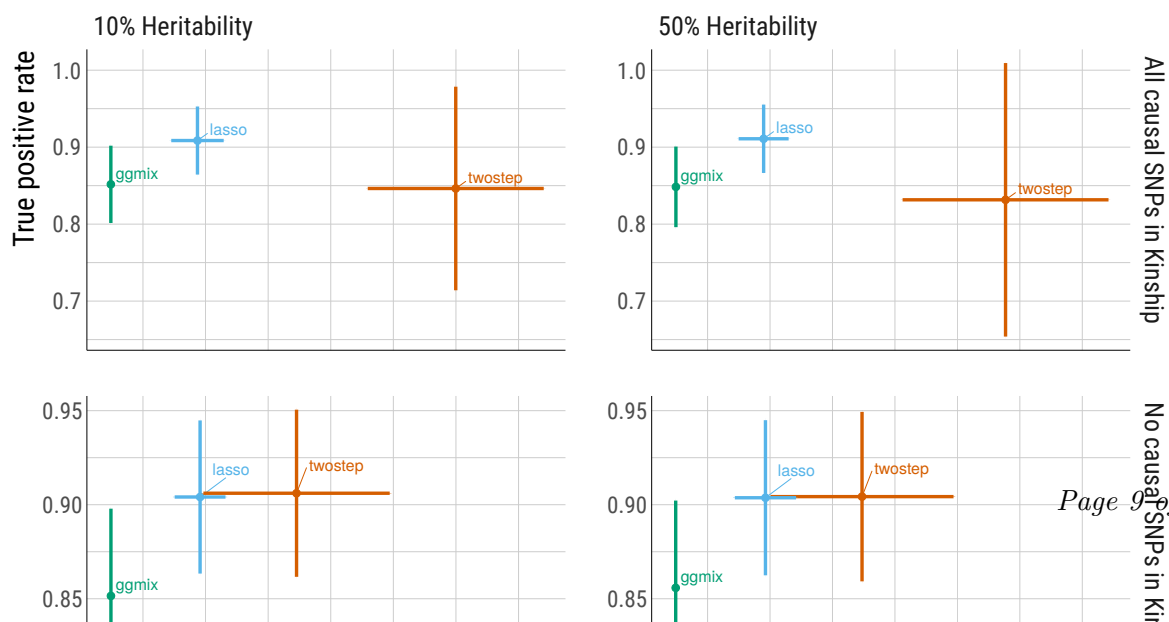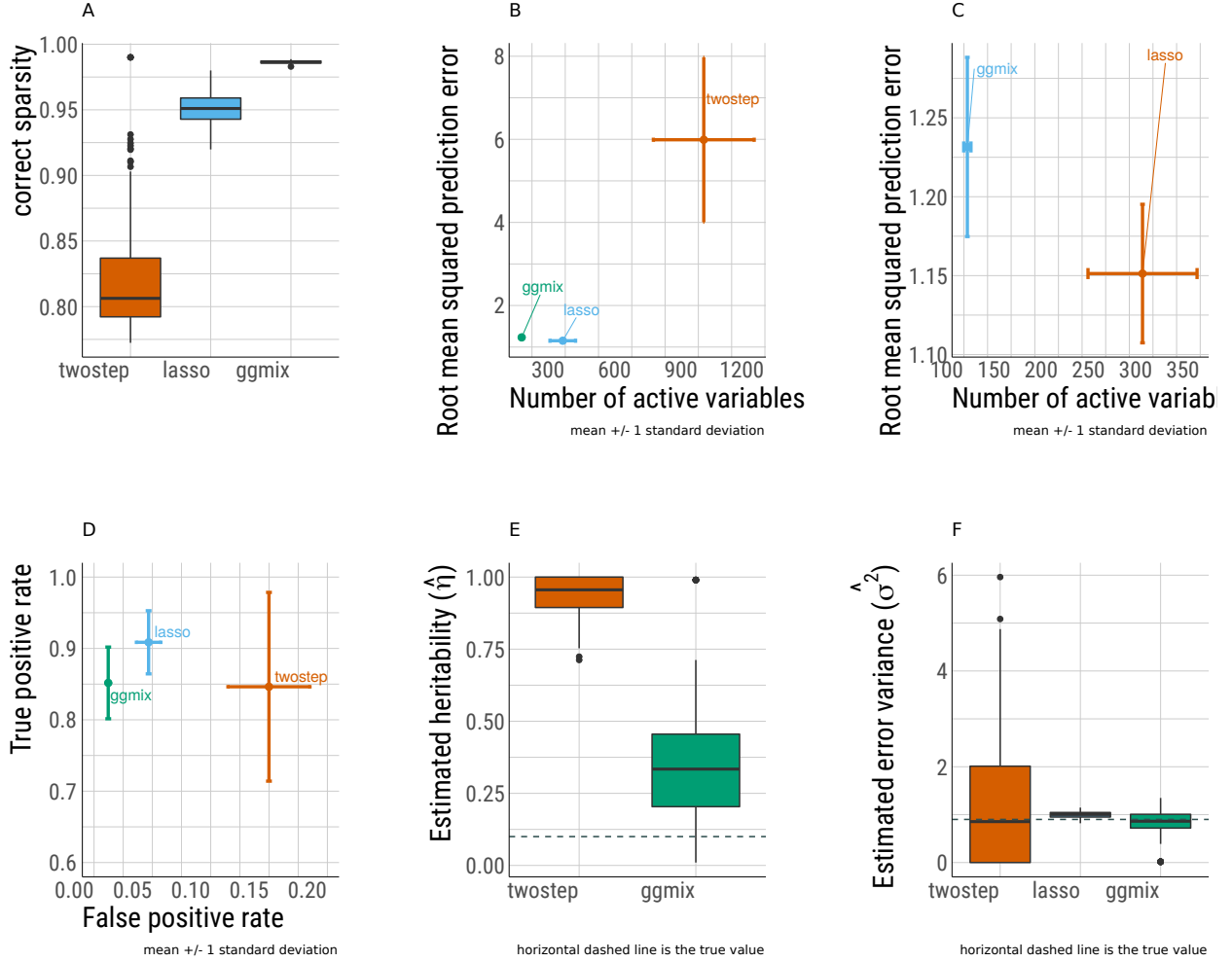
Based on 200 simulations

Figure 1: Boxplots of the correct sparsity from 200 simulations by the true heritability $\eta = \{10\%, 50\%\}$ and number of causal SNPs that were included in the calculation of the kinship matrix for the model with 1% causal SNPs ($c = 0.01$).

True Positive Rate vs. False Positive Rate (Mean +/- 1 SD) for the Model with 1% Causal SNPs

Based on 200 simulations

Figure 2: Boxplots of the correct sparsity from 200 simulations by the true heritability $\eta = \{10\%, 50\%\}$ and number of causal SNPs that were included in the calculation of the kinship matrix for the model with 1% causal SNPs ($c = 0.01$).

168 We plot the twostep and `ggmix` heritability estimates for $c = 0$ (Figure 18, Supplemental

169 Section B) and $c = 0.01$ (Figure 4). We see that both methods correctly estimate the

170 heritability in the null model. When all of the causal SNPs are in the kinship matrix, both

171 methods overestimate η though `ggmix` is closer to the true value. When none of the causal

172 SNPs are in the kinship, both methods tend to overestimate the truth when $\eta = 10\%$ and

173 underestimate when $\eta = 50\%$.

Estimated Heritability for the Model with 1% Causal SNPs
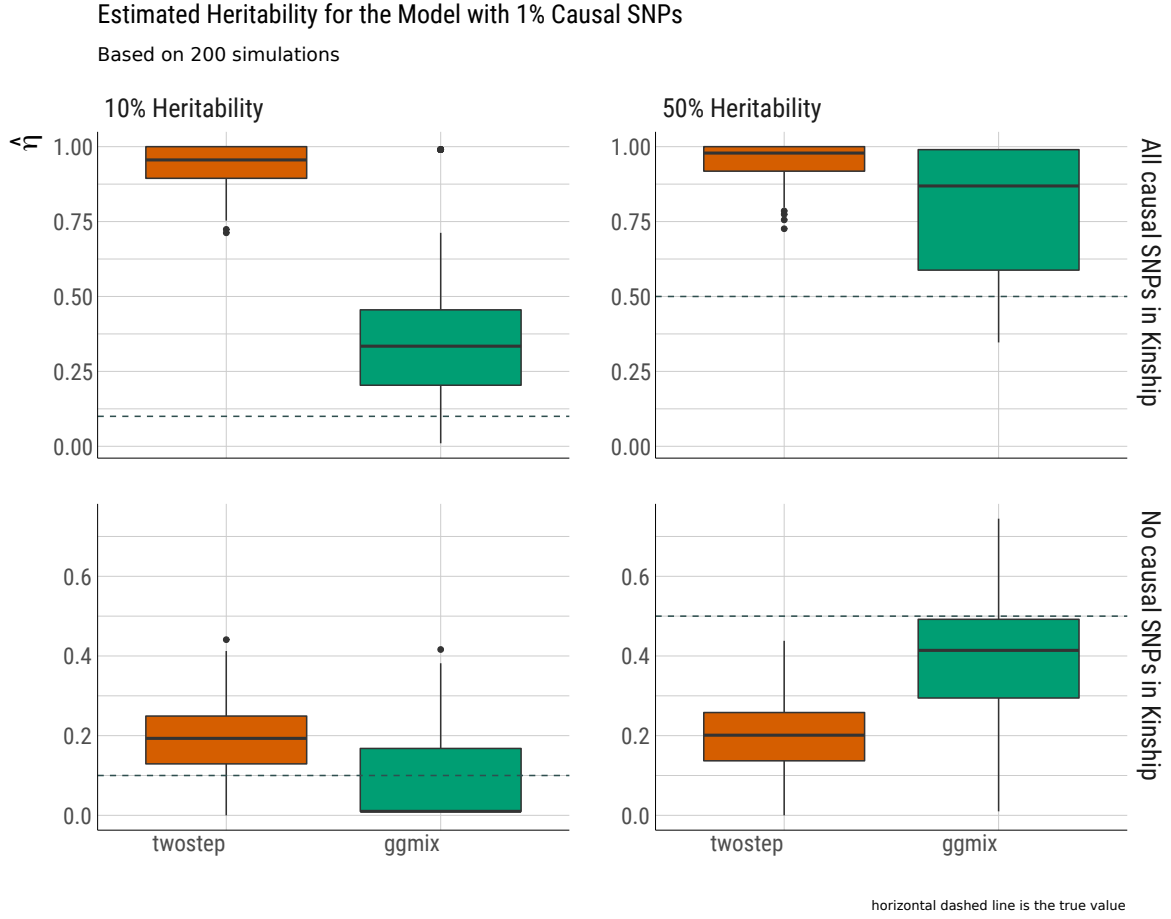
Based on 200 simulations

Figure 4: Boxplots of the heritability estimate $\hat{\eta}$ from 200 simulations by the true heritability $\eta = \{10\%, 50\%\}$ and number of causal SNPs that were included in the calculation of the kinship matrix for the model with 1% causal SNPs ($c = 0.01$).

In Figures 19 (Supplemental Section B) and 5, we plot the error variance for $c = 0$ and $c = 0.01$, respectively. The twostep and `ggmix` methods correctly estimate the error variance while the lasso overestimates it for the null model and for when 1% of the causal SNPs are in the kinship matrix. We see an inflated estimated error variance across all three methods when $c = 0.01$ and none of the causal SNPs are in the kinship matrix with the lasso and `ggmix` performing similarly.

Estimated Error Variance for the Model with 1% Causal SNPs
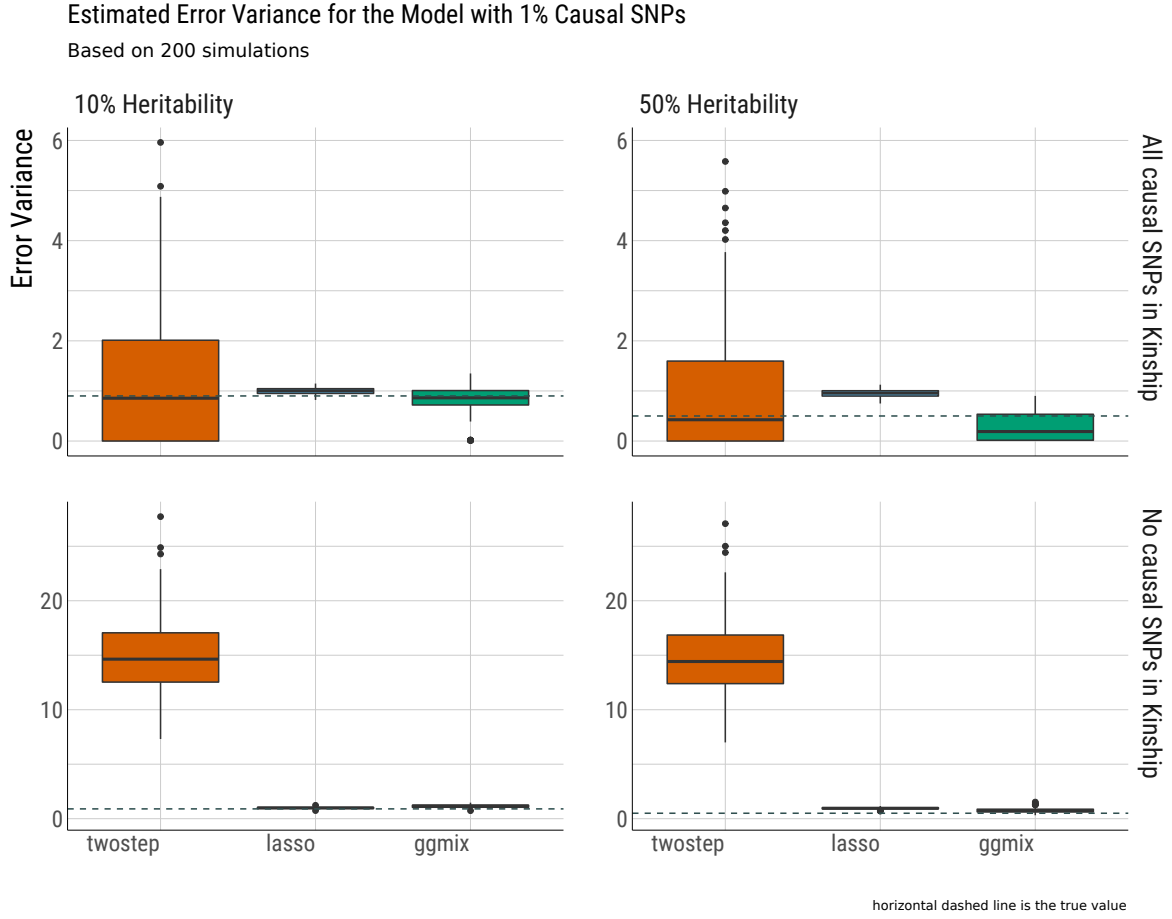
Based on 200 simulations

Figure 5: Boxplots of the estimated error variance from 200 simulations by the true heritability $\eta = \{10\%, 50\%\}$ and number of causal SNPs that were included in the calculation of the kinship matrix for the model with 1% causal SNPs ($c = 0.01$).

We compare the model error as a function of $\widehat{S}_{\hat{\lambda}}$ in Figures 20 (Supplemental Section B) and 6 for $c = 0$ and $c = 0.01$, respectively. Lasso achieves the smallest model error across all scenarios (for $c = 0.01$), albeit with a large number of active variables. ggmix has a smaller model error compared to twostep when all causal SNPs are in the kinship matrix and similar performance when none of the causal SNPs are in the kinship matrix.

Model Error vs. Number of Active Variable (Mean +/- 1 SD) for Model with 1% Causal SNPs

Based on 200 simulations

Figure 6: Means ± 1 standard deviation of the model error vs. the number of active variables by the true heritability $\eta = \{10\%, 50\%\}$ and number of causal SNPs that were included in the calculation of the kinship matrix for the model with 1% causal SNPs ($c = 0.01$).

Overall, we observe that variable selection results for `ggmix` are similar regardless of whether the causal SNPs are in the kinship matrix or not. This result is encouraging since in practice the kinship matrix is constructed from a random sample of SNPs across the genome, some of which are likely to be causal. `ggmix` has very good Type 1 error control, while both the lasso and twostep have a very high false positive rate. Inclusion of the causal SNPs in the kinship calculation has a strong impact on the variance component estimation with the heritabilty and error variance estimates working in opposite directions. That is, when all causal SNPs are in the kinship matrix, the heritability estimates are biased towards 1

while the error variance is correctly estimated. Conversely, when none of the causal SNPs are included in the kinship matrix, the estimated heritability is closer to the true value, while the error variance is inflated. Both the lasso and twostep methods have better signal recovery as compared to `ggmix`. However, this signal is being spread across many variables leading to many Type 1 errors.
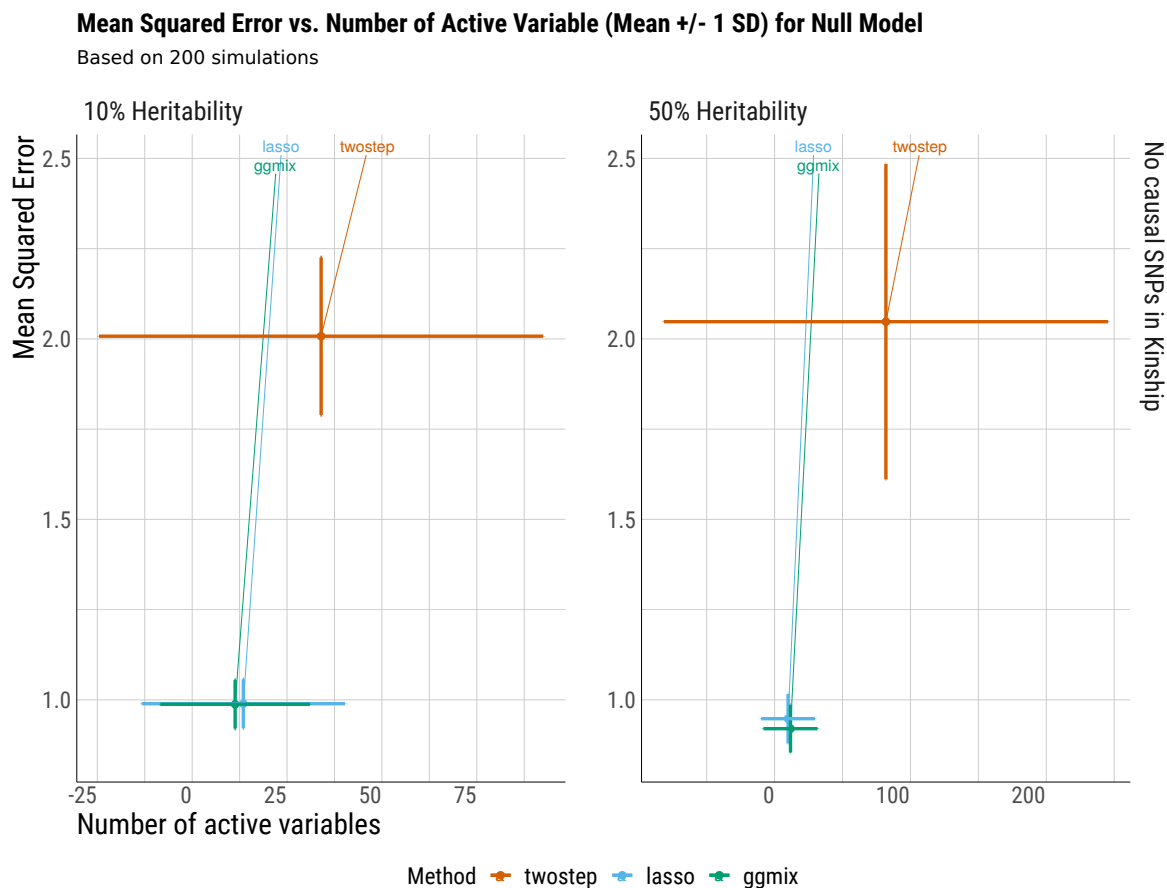

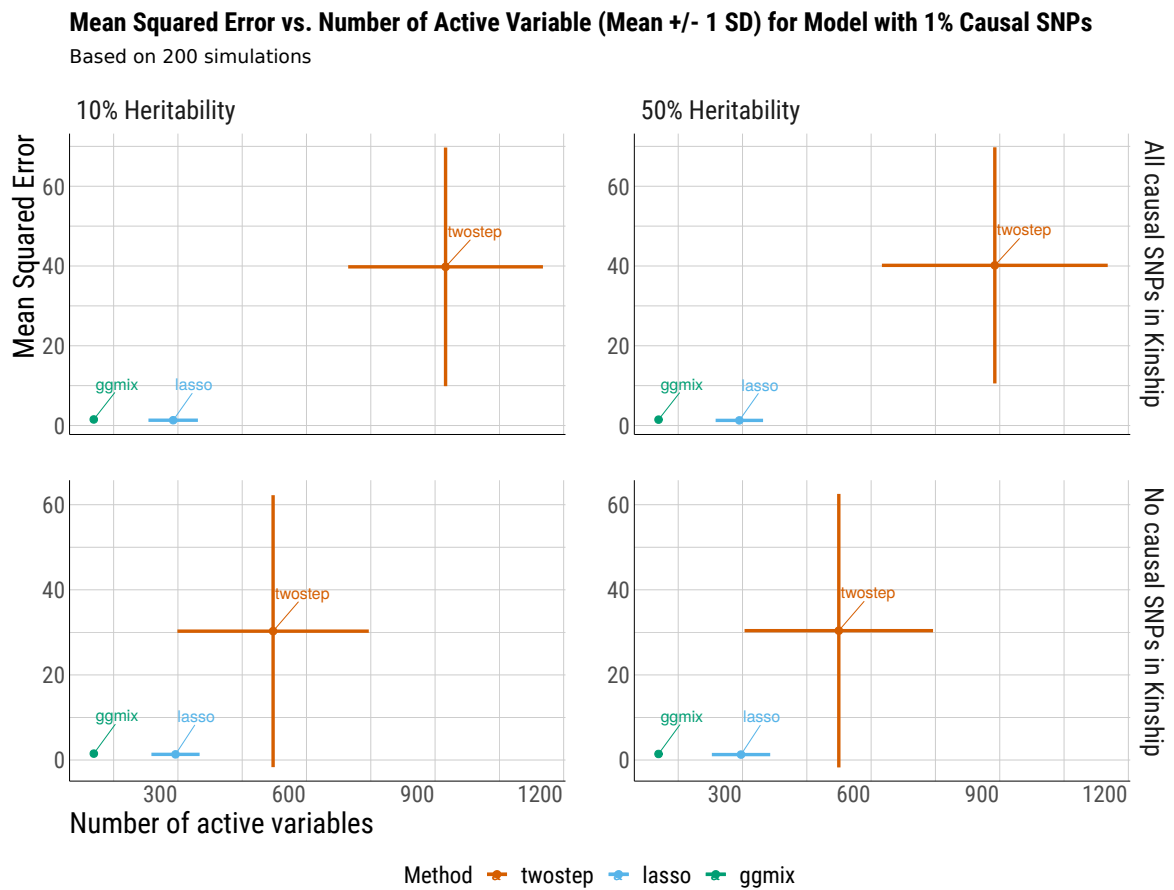Figure 7: Mean squared error vs number of active variables results for the null model.

Figure 8: Mean squared error vs number of active variables results for the model with 1% causal SNPs.
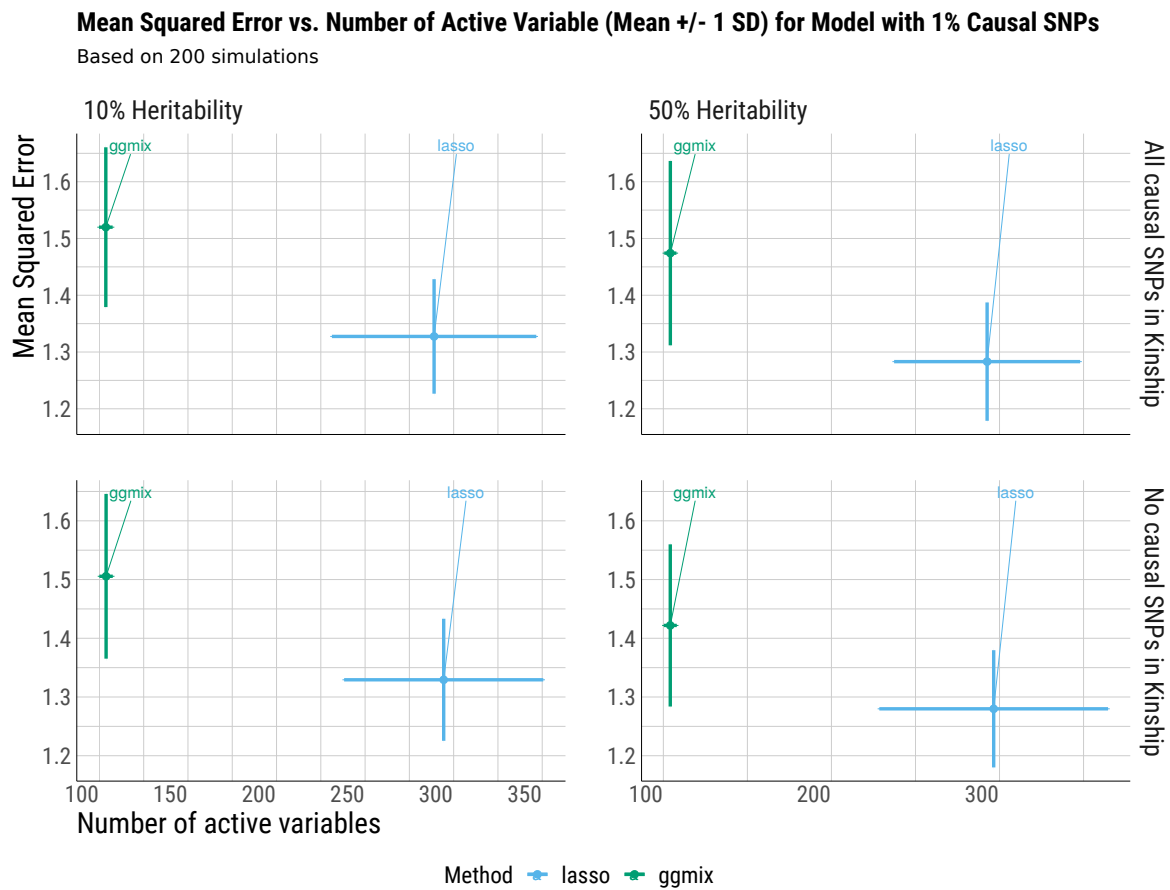
Figure 9: Mean squared error vs number of active variables results for 1% causal SNPs for ggmix and lasso.
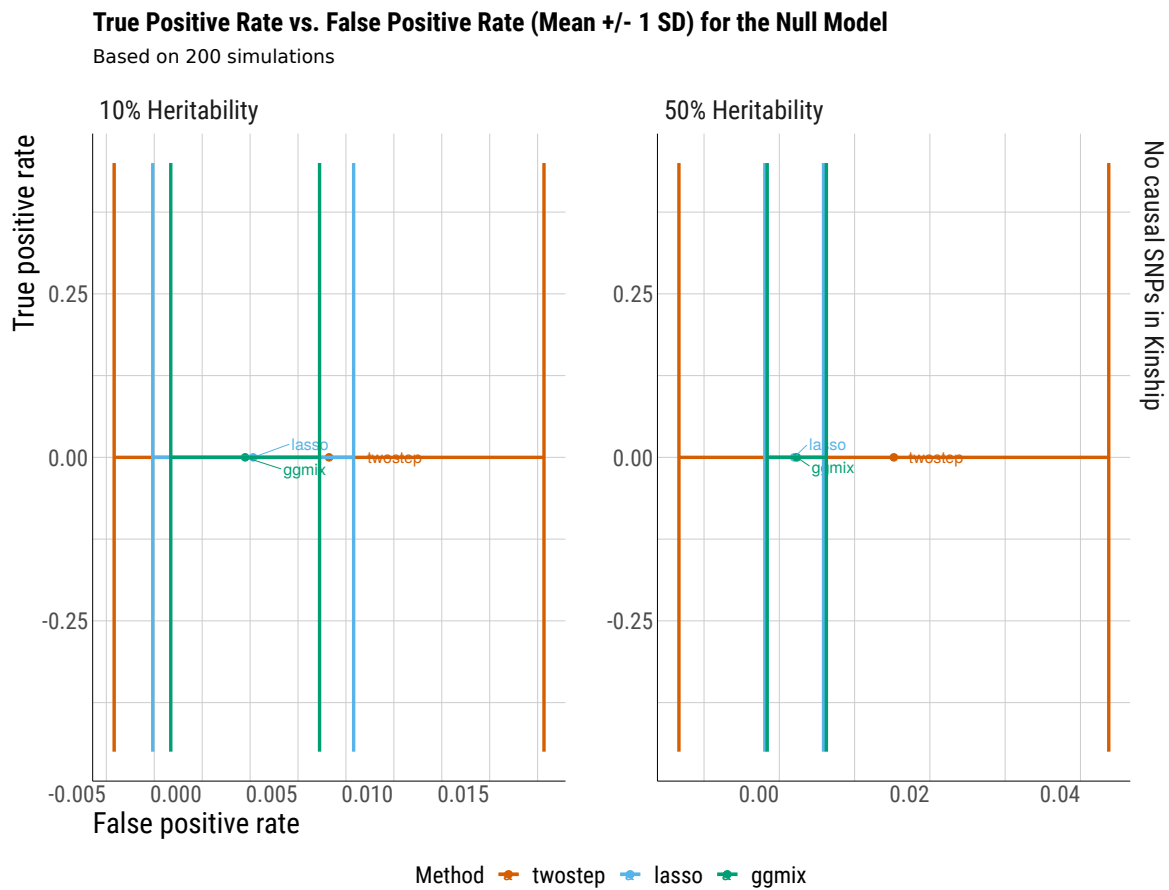
True Positive Rate vs. False Positive Rate (Mean +/- 1 SD) for the Null Model

Based on 200 simulations

Figure 10: Means ±1 standard deviation of true positive rate vs. false positive rate from 200 simulations by kinship geography and number of causal SNPs that were included in the calculation of the kinship matrix.
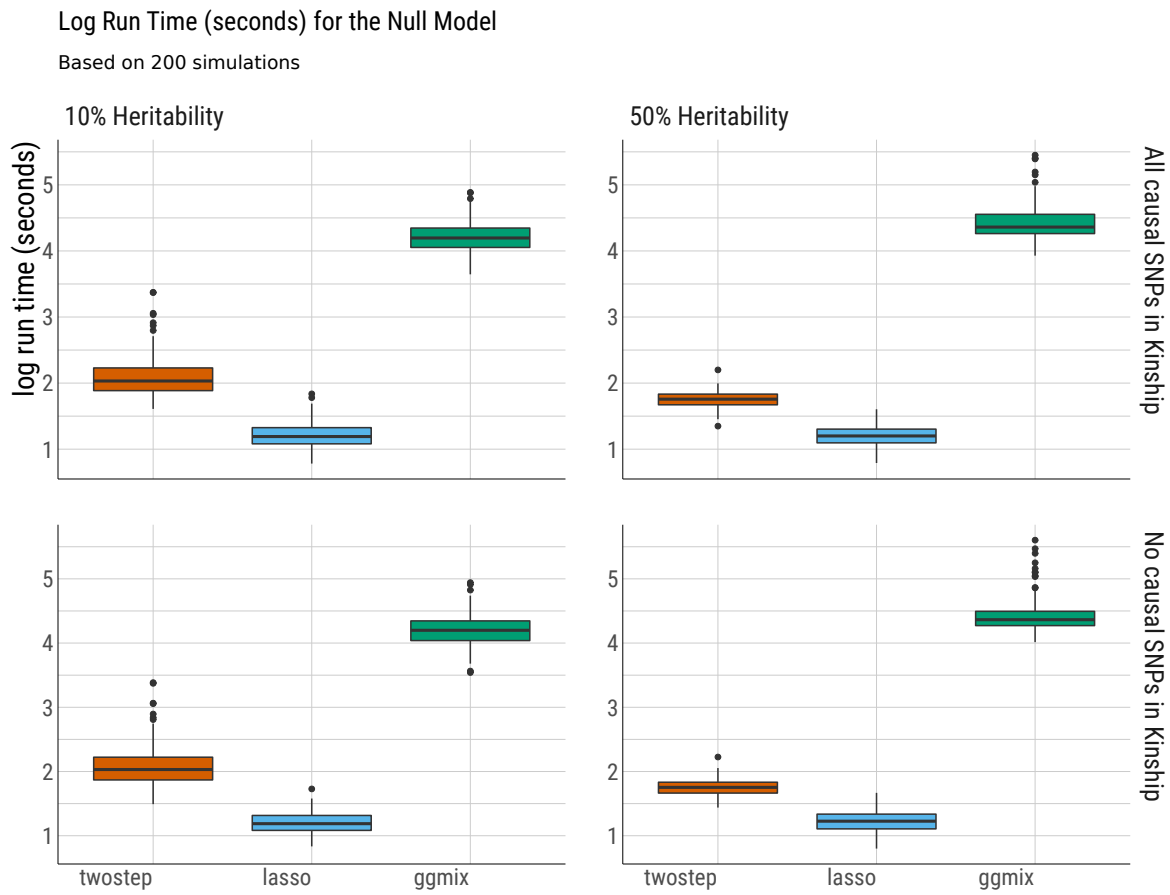
3.2   Run time

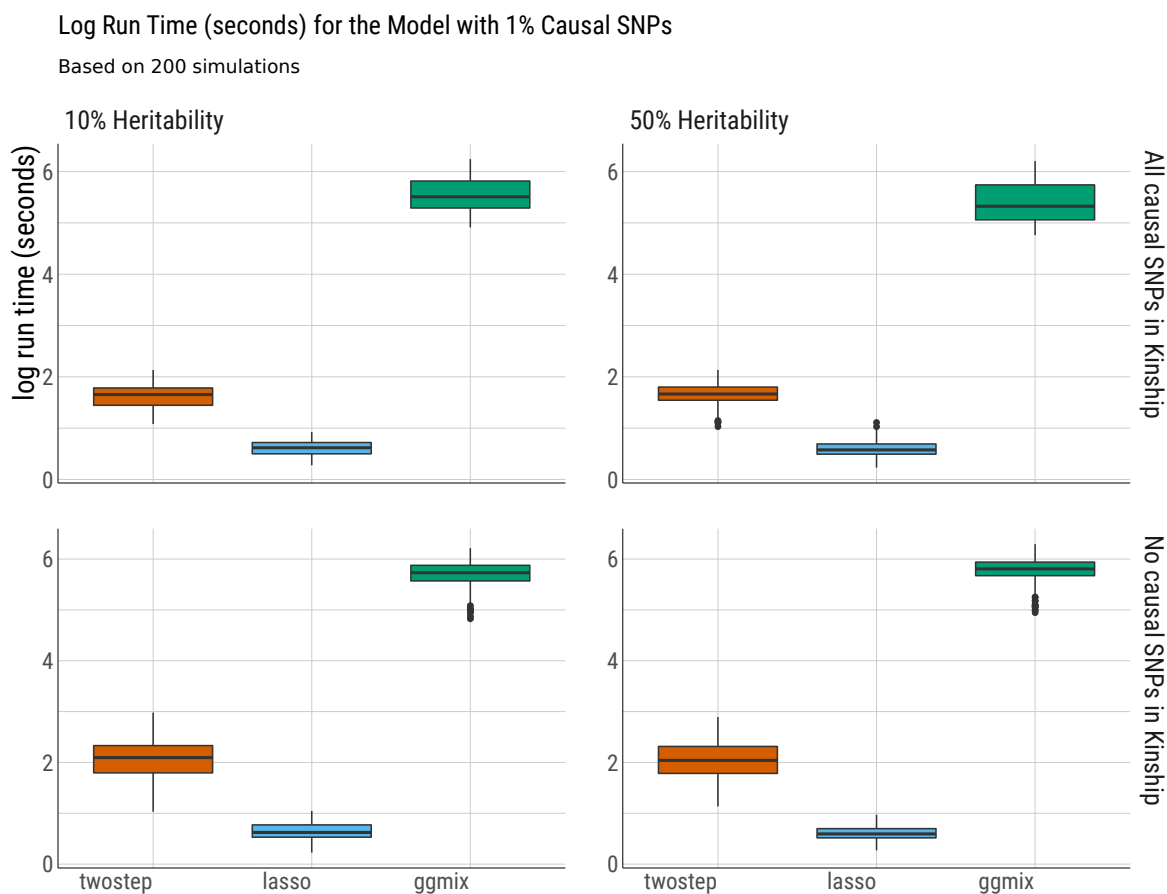Figure 11: Run time (in log seconds) for null model for twostep, lasso and ggmix.

Figure 12: Run time (in log seconds) for 1% causal SNPs for twostep, lasso and ggmix.

3.3   Real Data Application

Two datasets are used to illustrate `ggmix` has the potential with contrasting features. In one dataset, family strature induces low level of correlation and sparsity in signals. In the second mouse crosses, correlations are extremely strong and can confound signals.

3.3.1   GAW20

In the most recent Genetic Analysis Workshop 20 (GAW20), the causal modeling group investigated causal relationships between DNA methylation (exposure) within some genes and

the change in high-density lipoproteins ΔHDL (outcome) using Mendelian randomization (MR) [29]. Penalized regression methods could be used to select SNPs strongly associated with the exposure in order to be used as an instrumental variable (IV). However, since GAW20 data consisted of families, twostep methods were used which could have resulted in a large number of false positives. `ggmix` is an alternative approach that could be used for selecting the IV while accounting for the family structure of the data.

We applied `ggmix` to all 200 GAW20 simulation datasets, each of 679 observations, and compared its performance to the twostep and lasso methods. Using a FaST-LMM (Factored Spectrally Transformed Linear Mixed Model) [30], we validated the effect of rs9661059 on blood lipid trait to be significant (genome-wide $p = 6.29 \times 10^{-9}$). Though several other SNPs are also associated with the phenotype, these associations are probably mediated by CpG-SNP interaction pairs and do not reach statistical significance. Therefore, to avoid ambiguity, we only focused on chromosome 1 containing 51,104 SNPs where rs9661059 resides. Having acknowledged potential population admixture in the GAW20 study, we estimated the population kinship using REAP [31] after decomposing population compositions using ADMIXTURE [32]. We supplied the estimated kinship matrix directly to `ggmix` . For both the lasso and twostep methods, we adopted the same strategies as described in our simulation study in section 3.1, supplying the same kinship matrix estimated by REAP.

On each simulated replicate, we calibrated the methods so that they could be easily compared by fixing true positive rate to 1 and then minimizing false positive rate. Hence, the selected SNP, rs9661059, is likely to be the true positive for each method, and non-causal SNPs are excluded to the greatest extent. All of the three mothods precisely choose the correct predictor without any false positives in more than half of the replicates, given the strong causal signal. When some false positives are selected, `ggmix` performs comparably to twostep, and the lasso tends to select more false positives (Figure 13). Moreover, we assessed the accuracy of phenotype prediction following methods in section 5.3.7. We ob-

₂₃₂ served that `ggmix` outperforms the twostep method without requiring more SNPs, while

₂₃₃ it achieves roughly the same prediction accuracy as lasso but with fewer non-causal SNPs
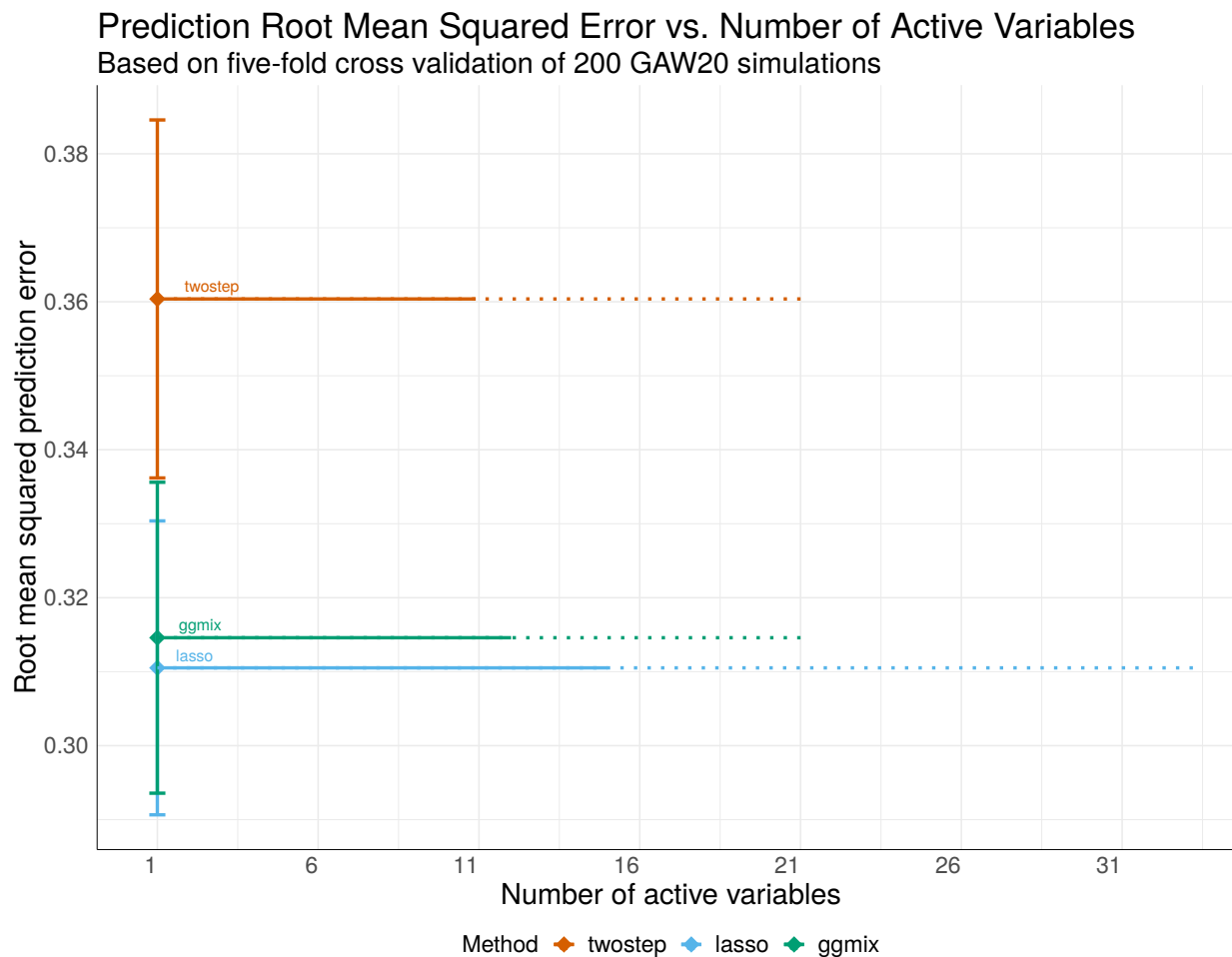
₂₃₄ (Figure 13).

Figure 13: Mean ±1 standard deviation of root mean square error vs. number of active variables used by each method. Diamonds represent median number of active variables and the corresponding root mean square error. Horizontal solid lines span from median to the 90th percentile; Horizontal dotted lines span from the 90th percentile to the 95th percentile.

₂₃₅ **3.3.2   Mouse Crosses**

₂₃₆ Mouse inbred strains of genetically identical individuals are extensively used in research.

₂₃₇ Crosses of different inbred strains are useful for various studies of heritability focusing on

either observable phenotypes or molecular mechanisms, and in particular, recombinant con-
genic strains have been an extremely useful resource for many years [33]. However, ignor-
ing complex genetic relationship in association studies can lead to inflated false positives
in genetic association studies when different inbred strains and their crosses are investi-
gated [34, 35, 36]. Therefore, a previous study developed and implemented a mixed model
to find loci associated with mouse sensitivity to mycobacterial infection [37]. The random
effects in the model captured complex correlation between the recombinant congenic mouse
strains based on the proportion of the shared identical by descent. Through a series of mixed
model fits at each marker, new loci on chromosome 1 and chromosome 11.

Here we show that `ggmix` can identify these loci, as well as potentially others, in a single
analysis. We also reanalyzed the mouse response to *Mycobacterium bovis* Bacille Calmette-
Guerin (BCG) Russia strain as reported in [37].

By taking the consensus between the "main model" and the "conditional model" of the origi-
nal study, we regarded markers D1Mit435 on chromosome 1 and D11Mit119 on chromosome
11 as two true positive loci. Similar to our aforementioned strategy of choosing the true
positives, we optimized models by tuning the penalty factor such that these two loci are
picked up, while the number of other active loci is minimized. To evaluate robustness of dif-
ferent models, we bootstrapped the 189-sample dataset and repeated analysis 200 times. We
directly estimated the kinship between mice using genotypes at 625 microsatellite markers.
The estimated kinship entered directly into `ggmix` and twostep. For the lasso, we calculated
and included the first 10 principal components of the estimated kinship. Significant markers
are defined as those captured in at least half of the bootstrap replicates, and in which the
corresponding method successfully captures both pre-selected true positives with a penalty
factor minimizing the number of active loci (Figure 14).

We demonstrate that `ggmix` recognizes the true associations more robustly than twostep and
lasso. In almost all (99%) bootstrap replicates, `ggmix` is able to capture both true positives,

₂₆₄ while twostep failed in 19% of the replicates and lasso failed in 56% of the replicates by

₂₆₅ missing of at least one of the two true positives (Figure 14). We also identified several other

₂₆₆ loci that might also be associated with susceptibility to myobacterial infection (Table 1).

₂₆₇ Among these new potentially-associated markders, D2Mit156 was found to play a role in

₂₆₈ control of parasite numbers of *Leishmania tropica* in lymph nodes [38]. This locus is con-

₂₆₉ sidered significant by our definition for both `ggmix` and lasso. An earlier study identified a

₂₇₀ parent-of-origin effect at D17Mit221 on CD4M levels [39]. This effect was more visible in

₂₇₁ crosses than in parental strains. In addition, D14Mit131, selected only by `ggmix` , was found

₂₇₂ to have a 9% loss of heterozygosity in hybrids of two inbred mouse strains [40], indicating the

₂₇₃ potential presence of putative suppressor genes pertaining to immune surveillance and tumor

₂₇₄ progression [41]. This result might also suggest association with anti-bacterial responses yet
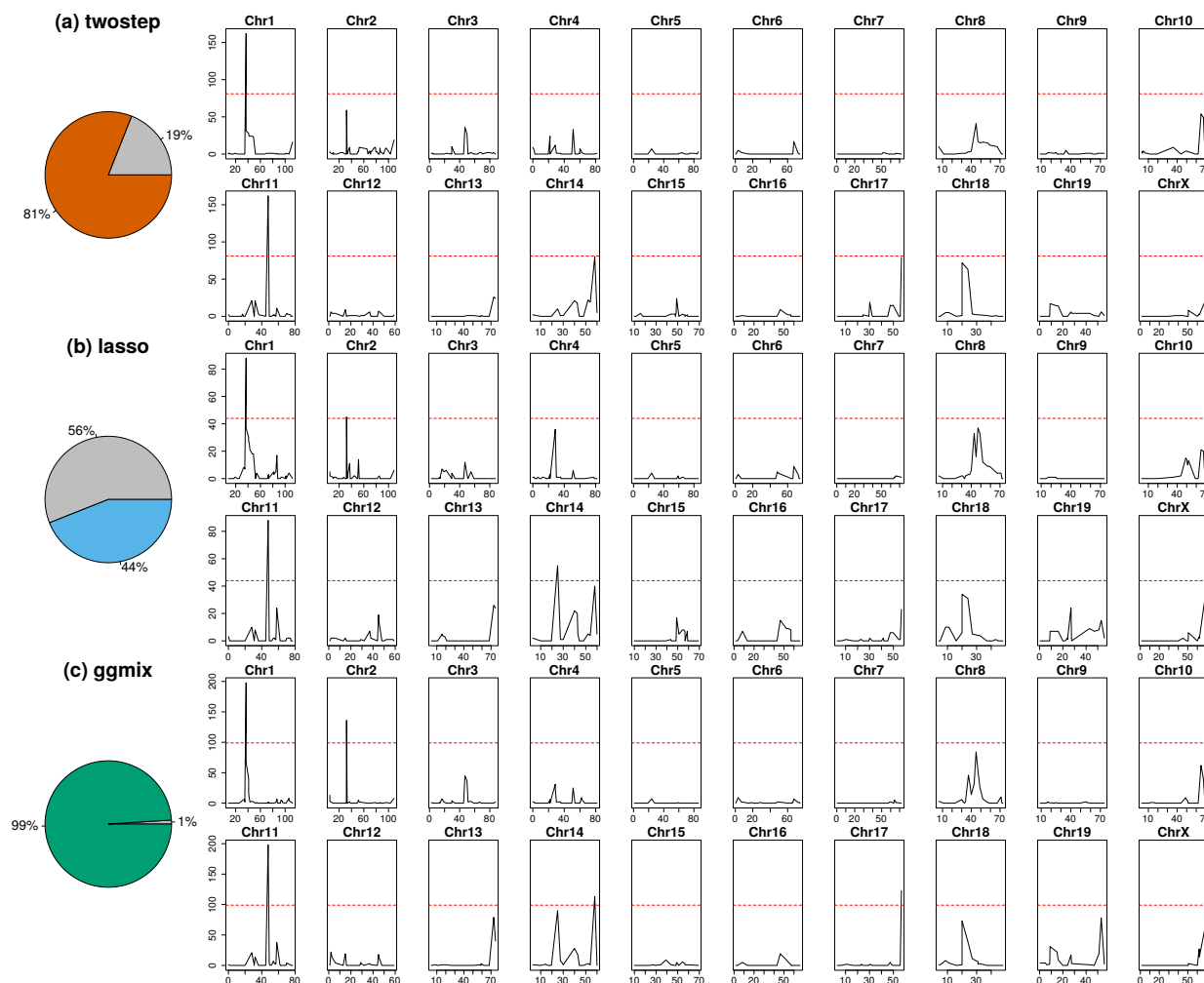
₂₇₅ to be discovered.

Figure 14: Comparison of model performance. Pie charts depict model robustness where grey areas denote bootstrap replicates on which the corresponding model is unable to capture both true positives using any penalty factor, whereas colored areas denote successful replicates. Chromosome-based signals record in how many successful replicates the corresponding loci are picked up by the corresponding optimized model. Red dashed lines delineate p value thresholds.

Table 1: Additional loci significantly associated with mouce susceptibility to myobacterial infection, after excluding two true positives. Loci needed to be identified in at least 50% of the successful bootstrap replicates that captured both true positive loci.

Method	Marker	Position in cM	Position in bp
twostep	N/A	N/A	N/A
lasso	D2Mit156	Chr2:31.66	Chr2:57081653-57081799
	D14Mit155	Chr14:31.52	Chr14:59828398-59828596
ggmix	D2Mit156	Chr2:31.66	Chr2:57081653-57081799
	D14Mit131	Chr14:63.59	Chr14:120006565-120006669
	D17Mit221	Chr17:59.77	Chr17:90087704-90087842

4   Discussion

We develop a general penalized LMM framework for population structure correction that simultaneously selects and estimates variables, accounting for between individual correlations, in one step. Our CGD algorithm is computationally efficient and has theoretical guarantees of convergence. We provide an easy-to-use software implementation of our algorithm along with a principled method for automatic tuning parameter selection. Through simulation studies, we show that existing approaches such as a two-stage approach or the lasso with a principal component adjustment lead to a large number of false positives. Our proposed method has excellent Type 1 error control and is robust to the inclusion of causal SNPs in the kinship matrix. This feature is important since in practice the kinship matrix is constructed from a random sample of SNPs across the genome, some of which are likely to be causal.

Although we derive a CGD algorithm for the ℓ_1 penalty, our approach can also be easily extended to other penalties such as the elastic net and group lasso with the same guarantees

of convergence.

A limitation of `ggmix` is that it first requires computing the covariance matrix with a computation time of $\mathcal{O}(n^2 k)$ followed by a spectral decomposition of this matrix in $\mathcal{O}(n^3)$ time where k is the number of SNP genotypes used to construct the covariance matrix. This computation becomes prohibitive for large cohorts such as the UK Biobank [42] which have collected genetic information on half a million individuals. When the matrix of genotypes used to construct the covariance matrix is low rank, there are additional computational speedups that can be implemented. While this has been developed for the univariate case [8], to our knowledge, this has not been explored in the multivariable case. We are currently developing a low rank version of the penalized LMM developed here, which reduces the time complexity from $\mathcal{O}(n^2 k)$ to $\mathcal{O}(n k^2)$.

While the predominant motivation for our approach has been association testing, we believe that there are other applications in which it can be used as well. For example, in the most recent Genetic Analysis Workshop 20 (GAW20), the causal modeling group investigated causal relationships between DNA methylation (exposure) within some genes and the change in high-density lipoproteins ΔHDL (outcome) using Mendelian randomization (MR) [29]. Penalized regression methods could be used to select SNPs strongly associated with the exposure in order to be used as an instrumental variable (IV). However, since GAW20 data consisted of families, two step methods were used which could have resulted in a large number of false positives. `ggmix` is an alternative approach that could be used for selecting the IV while accounting for the familial structure of the data. Our method is also suitable for fine mapping SNP association signals in genomic regions, where the goal is to pinpoint individual variants most likely to impact the undelying biological mechanisms of disease [43].

5 Materials and Methods

5.1 Model Set-up

Let $i = 1, \ldots, N$ be a grouping index, $j = 1, \ldots, n_i$ the observation index within a group and $N_T = \sum_{i=1}^{N} n_i$ the total number of observations. For each group let $\boldsymbol{y}_i = (y_1, \ldots, y_{n_i})$ be the observed vector of responses or phenotypes, $\mathbf{X}_i$ an $n_i \times (p + 1)$ design matrix (with the column of 1s for the intercept), $\boldsymbol{b}_i$ a group-specific random effect vector of length n_i and $\boldsymbol{\varepsilon}_i = (\varepsilon_{i1}, \ldots, \varepsilon_{in_i})$ the individual error terms. Denote the stacked vectors $\mathbf{Y} = (\boldsymbol{y}_i, \ldots, \boldsymbol{y}_N)^T \in \mathbb{R}^{N_T \times 1}$, $\boldsymbol{b} = (\boldsymbol{b}_i, \ldots, \boldsymbol{b}_N)^T \in \mathbb{R}^{N_T \times 1}$, $\boldsymbol{\varepsilon} = (\boldsymbol{\varepsilon}_i, \ldots, \boldsymbol{\varepsilon}_N)^T \in \mathbb{R}^{N_T \times 1}$, and the stacked matrix $\mathbf{X} = (\mathbf{X}_1, \ldots, \mathbf{X}_N)^T \in \mathbb{R}^{N_T \times (p+1)}$. Furthermore, let $\boldsymbol{\beta} = (\beta_0, \beta_1, \ldots, \beta_p)^T \in \mathbb{R}^{(p+1) \times 1}$ be a vector of fixed effects regression coefficients corresponding to $\mathbf{X}$. We consider the following linear mixed model with a single random effect [44]:

$$\mathbf{Y} = \mathbf{X}\boldsymbol{\beta} + \boldsymbol{b} + \boldsymbol{\varepsilon} \tag{2}$$

where the random effect $\boldsymbol{b}$ and the error variance $\boldsymbol{\varepsilon}$ are assigned the distributions

$$\boldsymbol{b} \sim \mathcal{N}(0, \eta\sigma^2\boldsymbol{\Phi}) \qquad \boldsymbol{\varepsilon} \sim \mathcal{N}(0, (1-\eta)\sigma^2\mathbf{I}) \tag{3}$$

Here, $\boldsymbol{\Phi}_{N_T \times N_T}$ is a known positive semi-definite and symmetric covariance or kinship matrix calculated from SNPs sampled across the genome, $\mathbf{I}_{N_T \times N_T}$ is the identity matrix and parameters σ^2 and $\eta \in [0, 1]$ determine how the variance is divided between $\boldsymbol{b}$ and $\boldsymbol{\varepsilon}$. Note that η is also the narrow-sense heritability (h^2), defined as the proportion of phenotypic variance attributable to the additive genetic factors [1]. The joint density of $\mathbf{Y}$ is therefore

multivariate normal:

$$\mathbf{Y}|(\boldsymbol{\beta}, \eta, \sigma^2) \sim \mathcal{N}(\mathbf{X}\boldsymbol{\beta}, \eta\sigma^2\boldsymbol{\Phi} + (1-\eta)\sigma^2\mathbf{I}) \tag{4}$$

The LMM-Lasso method [15] considers an alternative but equivalent parameterization given by:

$$\mathbf{Y}|(\boldsymbol{\beta}, \delta, \sigma_g^2) \sim \mathcal{N}(\mathbf{X}\boldsymbol{\beta}, \sigma_g^2(\boldsymbol{\Phi} + \delta\mathbf{I})) \tag{5}$$

where $\delta = \sigma_e^2/\sigma_g^2$, σ_g^2 is the genetic variance and σ_e^2 is the residual variance. We instead consider the parameterization in (4) since maximization is easier over the compact set $\eta \in [0, 1]$ than over the unbounded interval $\delta \in [0, \infty)$ [44]. We define the complete parameter vector as $\boldsymbol{\Theta} \coloneqq (\boldsymbol{\beta}, \eta, \sigma^2)$. The negative log-likelihood for (4) is given by

$$-\ell(\boldsymbol{\Theta}) \propto \frac{N_T}{2}\log(\sigma^2) + \frac{1}{2}\log\left(\det(\mathbf{V})\right) + \frac{1}{2\sigma^2}\left(\mathbf{Y} - \mathbf{X}\boldsymbol{\beta}\right)^T \mathbf{V}^{-1}\left(\mathbf{Y} - \mathbf{X}\boldsymbol{\beta}\right) \tag{6}$$

where $\mathbf{V} = \eta\boldsymbol{\Phi} + (1-\eta)\mathbf{I}$ and $\det(\mathbf{V})$ is the determinant of $\mathbf{V}$.

Let $\boldsymbol{\Phi} = \mathbf{U}\mathbf{D}\mathbf{U}^T$ be the eigen (spectral) decomposition of the kinship matrix $\boldsymbol{\Phi}$, where $\mathbf{U}_{N_T \times N_T}$ is an orthonormal matrix of eigenvectors (i.e. $\mathbf{U}\mathbf{U}^T = \mathbf{I}$) and $\mathbf{D}_{N_T \times N_T}$ is a diagonal matrix of eigenvalues Λ_i. $\mathbf{V}$ can then be further simplified [44]

$$\begin{aligned}
\mathbf{V} &= \eta\boldsymbol{\Phi} + (1-\eta)\mathbf{I} \\
&= \eta\mathbf{U}\mathbf{D}\mathbf{U}^T + (1-\eta)\mathbf{U}\mathbf{I}\mathbf{U}^T \\
&= \mathbf{U}\eta\mathbf{D}\mathbf{U}^T + \mathbf{U}(1-\eta)\mathbf{I}\mathbf{U}^T \\
&= \mathbf{U}\left(\eta\mathbf{D} + (1-\eta)\mathbf{I}\right)\mathbf{U}^T \\
&= \mathbf{U}\widetilde{\mathbf{D}}\mathbf{U}^T
\end{aligned} \tag{7}$$

where

$$\widetilde{\mathbf{D}} = \eta\mathbf{D} + (1 - \eta)\mathbf{I} \tag{8}$$

$$= \eta \begin{bmatrix} \Lambda_1 & & & \\ & \Lambda_2 & & \\ & & \ddots & \\ & & & \Lambda_{N_T} \end{bmatrix} + (1 - \eta) \begin{bmatrix} 1 & & & \\ & 1 & & \\ & & \ddots & \\ & & & 1 \end{bmatrix}$$

$$= \begin{bmatrix} 1 + \eta(\Lambda_1 - 1) & & & \\ & 1 + \eta(\Lambda_2 - 1) & & \\ & & \ddots & \\ & & & 1 + \eta(\Lambda_{N_T} - 1) \end{bmatrix}$$

$$= \operatorname{diag}\left\{1 + \eta(\Lambda_1 - 1), 1 + \eta(\Lambda_2 - 1), \ldots, 1 + \eta(\Lambda_{N_T} - 1)\right\} \tag{9}$$

Since (8) is a diagonal matrix, its inverse is also a diagonal matrix:

$$\widetilde{\mathbf{D}}^{-1} = \operatorname{diag}\left\{ \frac{1}{1 + \eta(\Lambda_1 - 1)}, \frac{1}{1 + \eta(\Lambda_2 - 1)}, \ldots, \frac{1}{1 + \eta(\Lambda_{N_T} - 1)} \right\} \tag{10}$$

From (7) and (9), $\log(\det(\mathbf{V}))$ simplifies to

$$\begin{aligned} \log(\det(\mathbf{V})) &= \log\left(\det(\mathbf{U})\det\left(\widetilde{\mathbf{D}}\right)\det(\mathbf{U}^T)\right) \\ &= \log\left\{ \prod_{i=1}^{N_T} (1 + \eta(\Lambda_i - 1)) \right\} \\ &= \sum_{i=1}^{N_T} \log(1 + \eta(\Lambda_i - 1)) \end{aligned} \tag{11}$$

since $\det(\mathbf{U}) = 1$. It also follows from (7) that

$$
\begin{aligned}
\mathbf{V}^{-1} &= \left(\mathbf{U}\widetilde{\mathbf{D}}\mathbf{U}^T\right)^{-1} \\
&= \left(\mathbf{U}^T\right)^{-1}\left(\widetilde{\mathbf{D}}\right)^{-1}\mathbf{U}^{-1} \\
&= \mathbf{U}\widetilde{\mathbf{D}}^{-1}\mathbf{U}^T
\end{aligned}
\tag{12}
$$

since for an orthonormal matrix $\mathbf{U}^{-1} = \mathbf{U}^T$. Substituting (10), (11) and (12) into (6) the negative log-likelihood becomes

$$
-\ell(\mathbf{\Theta}) \propto \frac{N_T}{2}\log(\sigma^2) + \frac{1}{2}\sum_{i=1}^{N_T}\log(1 + \eta(\Lambda_i - 1)) + \frac{1}{2\sigma^2}\left(\mathbf{Y} - \mathbf{X}\boldsymbol{\beta}\right)^T\mathbf{U}\widetilde{\mathbf{D}}^{-1}\mathbf{U}^T\left(\mathbf{Y} - \mathbf{X}\boldsymbol{\beta}\right)
\tag{13}
$$

$$
= \frac{N_T}{2}\log(\sigma^2) + \frac{1}{2}\sum_{i=1}^{N_T}\log(1 + \eta(\Lambda_i - 1)) + \frac{1}{2\sigma^2}\left(\mathbf{U}^T\mathbf{Y} - \mathbf{U}^T\mathbf{X}\boldsymbol{\beta}\right)^T\widetilde{\mathbf{D}}^{-1}\left(\mathbf{U}^T\mathbf{Y} - \mathbf{U}^T\mathbf{X}\boldsymbol{\beta}\right)
$$

$$
= \frac{N_T}{2}\log(\sigma^2) + \frac{1}{2}\sum_{i=1}^{N_T}\log(1 + \eta(\Lambda_i - 1)) + \frac{1}{2\sigma^2}\left(\widetilde{\mathbf{Y}} - \widetilde{\mathbf{X}}\boldsymbol{\beta}\right)^T\widetilde{\mathbf{D}}^{-1}\left(\widetilde{\mathbf{Y}} - \widetilde{\mathbf{X}}\boldsymbol{\beta}\right)
$$

$$
= \frac{N_T}{2}\log(\sigma^2) + \frac{1}{2}\sum_{i=1}^{N_T}\log(1 + \eta(\Lambda_i - 1)) + \frac{1}{2\sigma^2}\sum_{i=1}^{N_T}\frac{\left(\widetilde{Y}_i - \sum_{j=0}^{p}\widetilde{X}_{ij+1}\beta_j\right)^2}{1 + \eta(\Lambda_i - 1)}
\tag{14}
$$

where $\widetilde{\mathbf{Y}} = \mathbf{U}^T\mathbf{Y}$, $\widetilde{\mathbf{X}} = \mathbf{U}^T\mathbf{X}$, $\widetilde{Y}_i$ denotes the ith element of $\widetilde{\mathbf{Y}}$, $\widetilde{X}_{ij}$ is the i, j^{th} entry of $\widetilde{\mathbf{X}}$ and $\mathbf{1}$ is a column vector of N_T ones.

5.2   Penalized Maximum Likelihood Estimator

We define the $p + 3$ length vector of parameters $\mathbf{\Theta} := (\Theta_0, \Theta_1, \ldots, \Theta_{p+1}, \Theta_{p+2}, \Theta_{p+3}) = (\boldsymbol{\beta}, \eta, \sigma^2)$ where $\boldsymbol{\beta} \in \mathbb{R}^{p+1}, \eta \in [0, 1], \sigma^2 > 0$. In what follows, $p + 2$ and $p + 3$ are the indices in $\mathbf{\Theta}$ for η and σ^2, respectively. In light of our goals to select variables associated with the response in high-dimensional data, we propose to place a constraint on the magnitude of the regression coefficients. This can be achieved by adding a penalty term to the likelihood

function (14). The penalty term is a necessary constraint because in our applications, the sample size is much smaller than the number of predictors. We define the following objective function:

$$Q_\lambda(\mathbf{\Theta}) = f(\mathbf{\Theta}) + \lambda \sum_{j \neq 0} v_j P_j(\beta_j) \tag{15}$$

where $f(\mathbf{\Theta}) := -\ell(\mathbf{\Theta})$ is defined in (14), $P_j(\cdot)$ is a penalty term on the fixed regression coefficients $\beta_1, \ldots, \beta_{p+1}$ (we do not penalize the intercept) controlled by the nonnegative regularization parameter λ, and v_j is the penalty factor for jth covariate. These penalty factors serve as a way of allowing parameters to be penalized differently. Note that we do not penalize η or σ^2. An estimate of the regression parameters $\widehat{\mathbf{\Theta}}_\lambda$ is obtained by

$$\widehat{\mathbf{\Theta}}_\lambda = \arg\min_{\mathbf{\Theta}} Q_\lambda(\mathbf{\Theta}) \tag{16}$$

This is the general set-up for our model. In Section 5.3 we provide more specific details on how we solve (16).

5.3   Computational Algorithm

We use a general purpose block coordinate gradient descent algorithm (CGD) [45] to solve (16). At each iteration, we cycle through the coordinates and minimize the objective function with respect to one coordinate only. For continuously differentiable $f(\cdot)$ and convex and block-separable $P(\cdot)$ (i.e. $P(\boldsymbol{\beta}) = \sum_i P_i(\beta_i)$), Tseng and Yun [45] show that the solution generated by the CGD method is a stationary point of $Q_\lambda(\cdot)$ if the coordinates are updated in a Gauss-Seidel manner i.e. $Q_\lambda(\cdot)$ is minimized with respect to one parameter while holding all others fixed. The CGD algorithm has been successfully applied in fixed effects models (e.g. [46], [20]) and linear mixed models with an ℓ_1 penalty [47]. In the next section we provide some brief details about Algorithm 1. A more thorough treatment of the algorithm is given in Appendix A.

365 We emphasize here that previously developed methods such as the LMM-lasso [15] use a two-

366 stage fitting procedure without any convergence details. From a practical point of view, there

367 is currently no implementation that provides a principled way of determining the sequence

368 of tuning parameters to fit, nor a procedure that automatically selects the optimal value of

369 λ. To our knowledge, we are the first to develop a CGD algorithm in the specific context of

370 fitting a penalized LMM for population structure correction with theoretical guarantees of

371 convergence. Furthermore, we develop a principled method for automatic tuning parameter

372 selection and provide an easy-to-use software implementation in order to promote wider

373 uptake of these more complex methods by applied practitioners.

Algorithm 1: Block Coordinate Gradient Descent

Set the iteration counter $k \leftarrow 0$, initial values for the parameter vector $\boldsymbol{\Theta}^{(0)}$ and
convergence threshold ϵ;

for $\lambda \in \{\lambda_{max}, \ldots, \lambda_{min}\}$ **do**

    repeat

$$\boldsymbol{\beta}^{(k+1)} \leftarrow \arg\min_{\boldsymbol{\beta}} Q_\lambda \left(\boldsymbol{\beta}, \eta^{(k)}, \sigma^{2\,(k)} \right)$$

$$\eta^{(k+1)} \leftarrow \arg\min_{\eta} Q_\lambda \left(\boldsymbol{\beta}^{(k+1)}, \eta, \sigma^{2\,(k)} \right)$$

$$\sigma^{2\,(k+1)} \leftarrow \arg\min_{\sigma^2} Q_\lambda \left(\boldsymbol{\beta}^{(k+1)}, \eta^{(k+1)}, \sigma^2 \right)$$

       $k \leftarrow k + 1$

    until *convergence criterion is satisfied:* $\left\| \boldsymbol{\Theta}^{(k+1)} - \boldsymbol{\Theta}^{(k)} \right\|_2 < \epsilon$;

end

5.3.1   Updates for the β parameter

375 Recall that the part of the objective function that depends on $\boldsymbol{\beta}$ has the form

$$Q_\lambda(\boldsymbol{\Theta}) = \frac{1}{2} \sum_{i=1}^{N_T} w_i \left(\widetilde{Y}_i - \sum_{j=0}^{p} \widetilde{X}_{ij+1} \beta_j \right)^2 + \lambda \sum_{j=1}^{p} v_j |\beta_j| \tag{17}$$

376   where

$$w_i := \frac{1}{\sigma^2 \left(1 + \eta(\Lambda_i - 1)\right)} \tag{18}$$

Conditional on $\eta^{(k)}$ and $\sigma^{2\,(k)}$, it can be shown that the solution for β_j, $j = 1, \ldots, p$ is given by

$$\beta_j^{(k+1)} \leftarrow \frac{\mathcal{S}_\lambda \left(\sum_{i=1}^{N_T} w_i \widetilde{X}_{ij} \left(\widetilde{Y}_i - \sum_{\ell \neq j} \widetilde{X}_{i\ell} \beta_\ell^{(k)} \right) \right)}{\sum_{i=1}^{N_T} w_i \widetilde{X}_{ij}^2} \tag{19}$$

where $\mathcal{S}_\lambda(x)$ is the soft-thresholding operator

$$\mathcal{S}_\lambda(x) = \text{sign}(x)(|x| - \lambda)_+$$

377   $\text{sign}(x)$ is the signum function

$$\text{sign}(x) = \begin{cases} -1 & x < 0 \\ 0 & x = 0 \\ 1 & x > 0 \end{cases}$$

378   and $(x)_+ = \max(x, 0)$. We provide the full derivation in Appendix A.1.2.

5.3.2   Updates for the η paramter

379

380   Given $\boldsymbol{\beta}^{(k+1)}$ and $\sigma^{2\,(k)}$, solving for $\eta^{(k+1)}$ becomes a univariate optimization problem:

$$\eta^{(k+1)} \leftarrow \arg\min_\eta \frac{1}{2} \sum_{i=1}^{N_T} \log(1 + \eta(\Lambda_i - 1)) + \frac{1}{2\sigma^{2\,(k)}} \sum_{i=1}^{N_T} \frac{\left(\widetilde{Y}_i - \sum_{j=0}^{p} \widetilde{X}_{ij+1} \beta_j^{(k+1)} \right)^2}{1 + \eta(\Lambda_i - 1)} \tag{20}$$

381   We use a bound constrained optimization algorithm [48] implemented in the `optim` function

382   in `R` and set the lower and upper bounds to be 0.01 and 0.99, respectively.

5.3.3   Updates for the σ^2 parameter

Conditional on $\boldsymbol{\beta}^{(k+1)}$ and $\eta^{(k+1)}$, $\sigma^{2\,(k+1)}$ can be solved for using the following equation:

$$\sigma^{2\,(k+1)} \leftarrow \underset{\sigma^2}{\arg\min}\ \frac{N_T}{2}\log(\sigma^2) + \frac{1}{2\sigma^2}\sum_{i=1}^{N_T}\frac{\left(\widetilde{Y}_i - \sum_{j=0}^{p}\widetilde{X}_{ij+1}\beta_j\right)^2}{1+\eta(\Lambda_i-1)} \tag{21}$$

There exists an analytic solution for (21) given by:

$$\sigma^{2\,(k+1)} \leftarrow \frac{1}{N_T}\sum_{i=1}^{N_T}\frac{\left(\widetilde{Y}_i - \sum_{j=0}^{p}\widetilde{X}_{ij+1}\beta_j^{(k+1)}\right)^2}{1+\eta^{(k+1)}(\Lambda_i-1)} \tag{22}$$

5.3.4   Regularization path

In this section we describe how determine the sequence of tuning parameters λ at which to fit the model. Recall that our objective function has the form

$$Q_\lambda(\boldsymbol{\Theta}) = \frac{N_T}{2}\log(\sigma^2) + \frac{1}{2}\sum_{i=1}^{N_T}\log(1+\eta(\Lambda_i-1)) + \frac{1}{2}\sum_{i=1}^{N_T}w_i\left(\widetilde{Y}_i - \sum_{j=0}^{p}\widetilde{X}_{ij+1}\beta_j\right)^2 + \lambda\sum_{j=1}^{p}v_j|\beta_j| \tag{23}$$

The Karush-Kuhn-Tucker (KKT) optimality conditions for (23) are given by:

$$\begin{aligned}
\frac{\partial}{\partial\beta_1,\ldots,\beta_p}Q_\lambda(\boldsymbol{\Theta}) &= \mathbf{0}_p \\
\frac{\partial}{\partial\beta_0}Q_\lambda(\boldsymbol{\Theta}) &= 0 \\
\frac{\partial}{\partial\eta}Q_\lambda(\boldsymbol{\Theta}) &= 0 \\
\frac{\partial}{\partial\sigma^2}Q_\lambda(\boldsymbol{\Theta}) &= 0
\end{aligned} \tag{24}$$

389 The equations in (24) are equivalent to

$$\sum_{i=1}^{N_T} w_i \widetilde{X}_{i1} \left(\widetilde{Y}_i - \sum_{j=0}^{p} \widetilde{X}_{ij+1} \beta_j \right) = 0$$

$$\frac{1}{v_j} \sum_{i=1}^{N_T} w_i \widetilde{X}_{ij} \left(\widetilde{Y}_i - \sum_{j=0}^{p} \widetilde{X}_{ij+1} \beta_j \right) = \lambda \gamma_j,$$

$$\gamma_j \in \begin{cases} \text{sign}(\hat{\beta}_j) & \text{if} \quad \hat{\beta}_j \neq 0 \\ [-1,1] & \text{if} \quad \hat{\beta}_j = 0 \end{cases}, \qquad \text{for } j = 1,\dots,p \qquad (25)$$

$$\frac{1}{2} \sum_{i=1}^{N_T} \frac{\Lambda_i - 1}{1 + \eta(\Lambda_i - 1)} \left(1 - \frac{\left(\widetilde{Y}_i - \sum_{j=0}^{p} \widetilde{X}_{ij+1} \beta_j \right)^2}{\sigma^2 (1 + \eta(\Lambda_i - 1))} \right) = 0$$

$$\sigma^2 - \frac{1}{N_T} \sum_{i=1}^{N_T} \frac{\left(\widetilde{Y}_i - \sum_{j=0}^{p} \widetilde{X}_{ij+1} \beta_j \right)^2}{1 + \eta(\Lambda_i - 1)} = 0$$

390 where w_i is given by (18), $\widetilde{\mathbf{X}}_{-1}^{T}$ is $\widetilde{\mathbf{X}}^{T}$ with the first column removed, $\widetilde{\mathbf{X}}_{1}^{T}$ is the first column

391 of $\widetilde{\mathbf{X}}^{T}$, and $\boldsymbol{\gamma} \in \mathbb{R}^p$ is the subgradient function of the ℓ_1 norm evaluated at $(\hat{\beta}_1, \dots, \hat{\beta}_p)$.

392 Therefore $\widehat{\boldsymbol{\Theta}}$ is a solution in (16) if and only if $\widehat{\boldsymbol{\Theta}}$ satisfies (25) for some γ. We can determine

393 a decreasing sequence of tuning parameters by starting at a maximal value for $\lambda = \lambda_{max}$

394 for which $\hat{\beta}_j = 0$ for $j = 1, \dots, p$. In this case, the KKT conditions in (25) are equivalent

395 to

$$\frac{1}{v_j} \sum_{i=1}^{N_T} \left| w_i \widetilde{X}_{ij} \left(\widetilde{Y}_i - \widetilde{X}_{i1} \beta_0 \right) \right| \leq \lambda, \quad \forall j = 1, \dots, p$$

$$\beta_0 = \frac{\sum_{i=1}^{N_T} w_i \widetilde{X}_{i1} \widetilde{Y}_i}{\sum_{i=1}^{N_T} w_i \widetilde{X}_{i1}^2}$$

$$\frac{1}{2} \sum_{i=1}^{N_T} \frac{\Lambda_i - 1}{1 + \eta(\Lambda_i - 1)} \left(1 - \frac{\left(\widetilde{Y}_i - \widetilde{X}_{i1} \beta_0 \right)^2}{\sigma^2 (1 + \eta(\Lambda_i - 1))} \right) = 0 \qquad (26)$$

$$\sigma^2 = \frac{1}{N_T} \sum_{i=1}^{N_T} \frac{\left(\widetilde{Y}_i - \widetilde{X}_{i1} \beta_0 \right)^2}{1 + \eta(\Lambda_i - 1)}$$

396 We can solve the KKT system of equations in (26) (with a numerical solution for η) in order

to have an explicit form of the stationary point $\widehat{\boldsymbol{\Theta}}_0 = \left\{\hat{\beta}_0, \mathbf{0}_p, \hat{\eta}, \widehat{\sigma}^2\right\}$. Once we have $\widehat{\boldsymbol{\Theta}}_0$, we can solve for the smallest value of λ such that the entire vector $(\hat{\beta}_1, \ldots, \hat{\beta}_p)$ is 0:

$$\lambda_{max} = \max_j \left\{ \left| \frac{1}{v_j} \sum_{i=1}^{N_T} \hat{w}_i \widetilde{X}_{ij} \left(\widetilde{Y}_i - \widetilde{X}_{i1} \hat{\beta}_0 \right) \right| \right\}, \quad j = 1, \ldots, p \tag{27}$$

Following Friedman et al. [20], we choose $\tau \lambda_{max}$ to be the smallest value of tuning parameters λ_{min}, and construct a sequence of K values decreasing from λ_{max} to λ_{min} on the log scale. The defaults are set to $K = 100$, $\tau = 0.01$ if $n < p$ and $\tau = 0.001$ if $n \geq p$.

5.3.5 Warm Starts

The way in which we have derived the sequence of tuning parameters using the KKT conditions, allows us to implement warm starts. That is, the solution $\widehat{\boldsymbol{\Theta}}$ for λ_k is used as the initial value $\boldsymbol{\Theta}^{(0)}$ for λ_{k+1}. This strategy leads to computational speedups and has been implemented in the `ggmix` R package.

5.3.6 Prediction of the random effects

We use an empirical Bayes approach (e.g. [49]) to predict the random effects $\boldsymbol{b}$. Let the maximum a posteriori (MAP) estimate be defined as

$$\widehat{\boldsymbol{b}} = \arg\max_{\boldsymbol{b}} f(\boldsymbol{b}|\mathbf{Y}, \boldsymbol{\beta}, \eta, \sigma^2) \tag{28}$$

where, by using Bayes rule, $f(\boldsymbol{b}|\mathbf{Y}, \boldsymbol{\beta}, \eta, \sigma^2)$ can be expressed as

$$
\begin{aligned}
f(\boldsymbol{b}|\mathbf{Y}, \boldsymbol{\beta}, \eta, \sigma^2) &= \frac{f(\mathbf{Y}|\boldsymbol{b}, \boldsymbol{\beta}, \eta, \sigma^2)\pi(\boldsymbol{b}|\eta, \sigma^2)}{f(\mathbf{Y}|\boldsymbol{\beta}, \eta, \sigma^2)} \\
&\propto f(\mathbf{Y}|\boldsymbol{b}, \boldsymbol{\beta}, \eta, \sigma^2)\pi(\boldsymbol{b}|\eta, \sigma^2) \\
&\propto \exp\left\{-\frac{1}{2\sigma^2}(\mathbf{Y} - \mathbf{X}\boldsymbol{\beta} - \boldsymbol{b})^T\mathbf{V}^{-1}(\mathbf{Y} - \mathbf{X}\boldsymbol{\beta} - \boldsymbol{b}) - \frac{1}{2\eta\sigma^2}\boldsymbol{b}^T\boldsymbol{\Phi}^{-1}\boldsymbol{b}\right\} \\
&= \exp\left\{-\frac{1}{2\sigma^2}\left[(\mathbf{Y} - \mathbf{X}\boldsymbol{\beta} - \boldsymbol{b})^T\mathbf{V}^{-1}(\mathbf{Y} - \mathbf{X}\boldsymbol{\beta} - \boldsymbol{b}) + \frac{1}{\eta}\boldsymbol{b}^T\boldsymbol{\Phi}^{-1}\boldsymbol{b}\right]\right\} \quad (29)
\end{aligned}
$$

Solving for (28) is equivalent to minimizing the exponent in (29):

$$
\widehat{\boldsymbol{b}} = \arg\min_{\boldsymbol{b}}\left\{(\mathbf{Y} - \mathbf{X}\boldsymbol{\beta} - \boldsymbol{b})^T\mathbf{V}^{-1}(\mathbf{Y} - \mathbf{X}\boldsymbol{\beta} - \boldsymbol{b}) + \frac{1}{\eta}\boldsymbol{b}^T\boldsymbol{\Phi}^{-1}\boldsymbol{b}\right\} \quad (30)
$$

Taking the derivative of (30) with respect to $\boldsymbol{b}$ and setting it to 0 we get:

$$
\begin{aligned}
0 &= -2\mathbf{V}^{-1}(\mathbf{Y} - \mathbf{X}\boldsymbol{\beta} - \boldsymbol{b}) + \frac{2}{\eta}\boldsymbol{\Phi}^{-1}\boldsymbol{b} \\
&= -\mathbf{V}^{-1}(\mathbf{Y} - \mathbf{X}\boldsymbol{\beta}) + \left(\mathbf{V}^{-1} + \frac{1}{\eta}\boldsymbol{\Phi}^{-1}\right)\boldsymbol{b} \\
\widehat{\boldsymbol{b}} &= \left(\mathbf{V}^{-1} + \frac{1}{\widehat{\eta}}\boldsymbol{\Phi}^{-1}\right)^{-1}\mathbf{V}^{-1}(\mathbf{Y} - \mathbf{X}\widehat{\boldsymbol{\beta}}) \\
&= \left(\mathbf{U}\widetilde{\mathbf{D}}^{-1}\mathbf{U}^T + \frac{1}{\widehat{\eta}}\mathbf{U}\mathbf{D}^{-1}\mathbf{U}^T\right)^{-1}\mathbf{U}\widetilde{\mathbf{D}}^{-1}\mathbf{U}^T(\mathbf{Y} - \mathbf{X}\widehat{\boldsymbol{\beta}}) \\
&= \left(\mathbf{U}\left[\widetilde{\mathbf{D}}^{-1} + \frac{1}{\widehat{\eta}}\mathbf{D}^{-1}\right]\mathbf{U}^T\right)^{-1}\mathbf{U}\widetilde{\mathbf{D}}^{-1}(\widetilde{\mathbf{Y}} - \widetilde{\mathbf{X}}\widehat{\boldsymbol{\beta}}) \\
&= \mathbf{U}\left[\widetilde{\mathbf{D}}^{-1} + \frac{1}{\widehat{\eta}}\mathbf{D}^{-1}\right]^{-1}\mathbf{U}^T\mathbf{U}\widetilde{\mathbf{D}}^{-1}(\widetilde{\mathbf{Y}} - \widetilde{\mathbf{X}}\widehat{\boldsymbol{\beta}})
\end{aligned}
$$

where $\mathbf{V}^{-1}$ is given by (12), and $(\widehat{\boldsymbol{\beta}}, \widehat{\eta})$ are the estimates obtained from Algorithm 1.

5.3.7 Phenotype prediction

Here we describe the method used for predicting the unobserved phenotype $\mathbf{Y}^\star$ in a set of individuals with predictor set $\mathbf{X}^\star$ that were not used in the model training e.g. a testing

set. Let q denote the number of observations in the testing set and $N - q$ the number of observations in the training set. We assume that a `ggmix` model has been fit on a set of training individuals with observed phenotype $\mathbf{Y}$ and predictor set $\mathbf{X}$. We further assume that $\mathbf{Y}$ and $\mathbf{Y}^\star$ are jointly multivariate Normal:

$$\begin{bmatrix} \mathbf{Y}^\star \\ \mathbf{Y} \end{bmatrix} \sim \mathcal{N} \left(\begin{bmatrix} \boldsymbol{\mu}_{1_{(q \times 1)}} \\ \boldsymbol{\mu}_{2_{(N-q) \times 1}} \end{bmatrix}, \begin{bmatrix} \boldsymbol{\Sigma}_{11_{(q \times q)}} & \boldsymbol{\Sigma}_{12_{q \times (N-q)}} \\ \boldsymbol{\Sigma}_{21_{(N-q) \times q}} & \boldsymbol{\Sigma}_{22_{(N-q) \times (N-q)}} \end{bmatrix} \right) \tag{31}$$

Then, from standard multivariate Normal theory, the conditional distribution $\mathbf{Y}^\star | \mathbf{Y}, \eta, \sigma^2, \boldsymbol{\beta}, \mathbf{X}, \mathbf{X}^\star$ is $\mathcal{N}(\boldsymbol{\mu}^\star, \boldsymbol{\Sigma}^\star)$ where

$$\boldsymbol{\mu}^\star = \boldsymbol{\mu}_1 + \boldsymbol{\Sigma}_{12} \boldsymbol{\Sigma}_{22}^{-1} (\mathbf{Y} - \mu_2) \tag{32}$$

$$\boldsymbol{\Sigma}^\star = \boldsymbol{\Sigma}_{11} - \boldsymbol{\Sigma}_{12} \boldsymbol{\Sigma}_{22}^{-1} \boldsymbol{\Sigma}_{21} \tag{33}$$

The phenotype prediction is thus given by:

$$\boldsymbol{\mu}^\star_{q \times 1} = \mathbf{X}^\star \boldsymbol{\beta} + \frac{1}{\sigma^2} \boldsymbol{\Sigma}_{12} \mathbf{V}^{-1} (\mathbf{Y} - \mathbf{X}\boldsymbol{\beta}) \tag{34}$$

$$= \mathbf{X}^\star \boldsymbol{\beta} + \frac{1}{\sigma^2} \boldsymbol{\Sigma}_{12} \mathbf{U} \widetilde{\mathbf{D}}^{-1} \mathbf{U}^T (\mathbf{Y} - \mathbf{X}\boldsymbol{\beta}) \tag{35}$$

$$= \mathbf{X}^\star \boldsymbol{\beta} + \frac{1}{\sigma^2} \boldsymbol{\Sigma}_{12} \mathbf{U} \widetilde{\mathbf{D}}^{-1} (\widetilde{\mathbf{Y}} - \widetilde{\mathbf{X}}\boldsymbol{\beta}) \tag{36}$$

$$= \mathbf{X}^\star \boldsymbol{\beta} + \frac{1}{\sigma^2} \eta \sigma^2 \boldsymbol{\Phi}^\star \mathbf{U} \widetilde{\mathbf{D}}^{-1} (\widetilde{\mathbf{Y}} - \widetilde{\mathbf{X}}\boldsymbol{\beta}) \tag{37}$$

$$= \mathbf{X}^\star \boldsymbol{\beta} + \eta \boldsymbol{\Phi}^\star \mathbf{U} \widetilde{\mathbf{D}}^{-1} (\widetilde{\mathbf{Y}} - \widetilde{\mathbf{X}}\boldsymbol{\beta}) \tag{38}$$

where $\boldsymbol{\Phi}^\star$ is the $q \times (N - q)$ covariance matrix between the testing and training individuals.

5.3.8 Choice of the optimal tuning parameter

In order to choose the optimal value of the tuning parameter λ, we use the generalized information criterion [50] (GIC):

$$GIC_\lambda = -2\ell(\widehat{\boldsymbol{\beta}}, \widehat{\sigma}^2, \widehat{\eta}) + a_n \cdot \widehat{df}_\lambda \tag{39}$$

where $\widehat{df}_\lambda$ is the number of non-zero elements in $\widehat{\boldsymbol{\beta}}_\lambda$ [51] plus two (representing the variance parameters η and σ^2). Several authors have used this criterion for variable selection in mixed models with $a_n = \log N_T$ [47, 52], which corresponds to the BIC. We instead choose the high-dimensional BIC [53] given by $a_n = \log(\log(N_T)) * \log(p)$. This is the default choice in our `ggmix` R package, though the interface is flexible to allow the user to select their choice of a_n.

Acknowledgments

References

[1] Manolio TA, Collins FS, Cox NJ, Goldstein DB, Hindorff LA, Hunter DJ, et al. Finding the missing heritability of complex diseases. Nature. 2009;461(7265):747. 2, 3, 27

[2] Yang J, Benyamin B, McEvoy BP, Gordon S, Henders AK, Nyholt DR, et al. Common SNPs explain a large proportion of the heritability for human height. Nature genetics. 2010;42(7):565. 2

[3] Astle W, Balding DJ, et al. Population structure and cryptic relatedness in genetic association studies. Statistical Science. 2009;24(4):451–471. 3

[4] Song M, Hao W, Storey JD. Testing for genetic associations in arbitrarily structured populations. Nature genetics. 2015;47(5):550–554. 3

[5] Marchini J, Cardon LR, Phillips MS, Donnelly P. The effects of human population structure on large genetic association studies. Nature genetics. 2004;36(5):512. 3

[6] Hoggart CJ, Whittaker JC, De Iorio M, Balding DJ. Simultaneous analysis of all SNPs in genome-wide and re-sequencing association studies. PLoS genetics. 2008;4(7):e1000130. 3

[7] Li J, Das K, Fu G, Li R, Wu R. The Bayesian lasso for genome-wide association studies. Bioinformatics. 2010;27(4):516–523. 3

[8] Lippert C, Listgarten J, Liu Y, Kadie CM, Davidson RI, Heckerman D. FaST linear mixed models for genome-wide association studies. Nature methods. 2011;8(10):833–835. 3, 7, 26

[9] Kang HM, Sul JH, Zaitlen NA, Kong Sy, Freimer NB, Sabatti C, et al. Variance component model to account for sample structure in genome-wide association studies. Nature genetics. 2010;42(4):348. 3

[10] Yu J, Pressoir G, Briggs WH, Bi IV, Yamasaki M, Doebley JF, et al. A unified mixed-model method for association mapping that accounts for multiple levels of relatedness. Nature genetics. 2006;38(2):203. 3

[11] Eu-Ahsunthornwattana J, Miller EN, Fakiola M, Jeronimo SM, Blackwell JM, Cordell HJ, et al. Comparison of methods to account for relatedness in genome-wide association studies with family-based data. PLoS Genet. 2014;10(7):e1004445. 3

[12] Price AL, Patterson NJ, Plenge RM, Weinblatt ME, Shadick NA, Reich D. Principal components analysis corrects for stratification in genome-wide association studies. Nature genetics. 2006;38(8):904. 3

[13] Oualkacha K, Dastani Z, Li R, Cingolani PE, Spector TD, Hammond CJ, et al. Adjusted sequence kernel association test for rare variants controlling for cryptic and family relatedness. Genetic epidemiology. 2013;37(4):366–376. 3, 4

[14] Cordell HJ, Clayton DG. A unified stepwise regression procedure for evaluating the relative effects of polymorphisms within a gene using case/control or family data: application to HLA in type 1 diabetes. The American Journal of Human Genetics. 2002;70(1):124–141. 4

[15] Rakitsch B, Lippert C, Stegle O, Borgwardt K. A Lasso multi-marker mixed model for association mapping with population structure correction. Bioinformatics. 2013;29(2):206–214. 4, 28, 32

[16] Wang D, Eskridge KM, Crossa J. Identifying QTLs and epistasis in structured plant populations using adaptive mixed LASSO. Journal of agricultural, biological, and environmental statistics. 2011;16(2):170–184. 4

[17] Tibshirani R. Regression shrinkage and selection via the lasso. Journal of the Royal Statistical Society Series B (Methodological). 1996;p. 267–288. 4

[18] Zou H. The adaptive lasso and its oracle properties. Journal of the American statistical association. 2006;101(476):1418–1429. 4

[19] Ding X, Su S, Nandakumar K, Wang X, Fardo DW. A 2-step penalized regression method for family-based next-generation sequencing association studies. In: BMC proceedings. vol. 8. BioMed Central; 2014. p. S25. 4

[20] Friedman J, Hastie T, Tibshirani R. Regularization paths for generalized linear models via coordinate descent. Journal of statistical software. 2010;33(1):1. 4, 6, 31, 36, 47

[21] Yang Y, Zou H. A fast unified algorithm for solving group-lasso penalize learning problems. Statistics and Computing. 2015;25(6):1129–1141. 4

[22] Yang J, Zaitlen NA, Goddard ME, Visscher PM, Price AL. Advantages and pitfalls in the application of mixed-model association methods. Nature genetics. 2014;46(2):100. 4

[23] Zou H, Hastie T. Regularization and variable selection via the elastic net. Journal of the Royal Statistical Society: Series B (Statistical Methodology). 2005;67(2):301–320. 4

[24] Yuan M, Lin Y. Model selection and estimation in regression with grouped variables. Journal of the Royal Statistical Society: Series B (Statistical Methodology). 2006;68(1):49–67. 4

[25] Gilmour AR, Thompson R, Cullis BR. Average information REML: an efficient algorithm for variance parameter estimation in linear mixed models. Biometrics. 1995;p. 1440–1450. 5

[26] Dandine-Roulland C. gaston: Genetic Data Handling (QC, GRM, LD, PCA) and Linear Mixed Models; 2018. R package version 1.5.3. Available from: https://CRAN.R-project.org/package=gaston. 5

[27] Ochoa A, Storey JD. FST and kinship for arbitrary population structures I: Generalized definitions. bioRxiv. 2016;. 7

[28] Ochoa A, Storey JD. FST and kinship for arbitrary population structures II: Method of moments estimators. bioRxiv. 2016;. 7

[29] Davey Smith G, Ebrahim S. Mendelian randomization: can genetic epidemiology contribute to understanding environmental determinants of disease? International journal of epidemiology. 2003;32(1):1–22. 20, 26

[30] Howey RA, Cordell HJ. Application of Bayesian networks to GAW20 genetic and blood lipid data. In: BMC proceedings. vol. 12. BioMed Central; 2018. p. 19. 20

[31] Thornton T, Tang H, Hoffmann TJ, Ochs-Balcom HM, Caan BJ, Risch N. Estimating kinship in admixed populations. The American Journal of Human Genetics. 2012;91(1):122–138. 20

[32] Alexander DH, Novembre J, Lange K. Fast model-based estimation of ancestry in unrelated individuals. Genome research. 2009;19(9):1655–1664. 20

[33] Fortin A, Diez E, Rochefort D, Laroche L, Malo D, Rouleau GA, et al. Recombinant congenic strains derived from A/J and C57BL/6J: a tool for genetic dissection of complex traits. Genomics. 2001;74(1):21–35. 22

[34] Bennett BJ, Farber CR, Orozco L, Kang HM, Ghazalpour A, Siemers N, et al. A high-resolution association mapping panel for the dissection of complex traits in mice. Genome research. 2010;20(2):281–290. 22

[35] Flint J, Eskin E. Genome-wide association studies in mice. Nature Reviews Genetics. 2012;13(11):807. 22

[36] Cheng R, Lim JE, Samocha KE, Sokoloff G, Abney M, Skol AD, et al. Genome-wide association studies and the problem of relatedness among advanced intercross lines and other highly recombinant populations. Genetics. 2010;185(3):1033–1044. 22

[37] Di Pietrantonio T, Hernandez C, Girard M, Verville A, Orlova M, Belley A, et al. Strain-specific differences in the genetic control of two closely related mycobacteria. PLoS pathogens. 2010;6(10):e1001169. 22

[38] Sohrabi Y, Havelková H, Kobets T, Šíma M, Volkova V, Grekov I, et al. Mapping the Genes for Susceptibility and Response to Leishmania tropica in Mouse. PLoS neglected tropical diseases. 2013;7(7):e2282. 23

[39] Jackson AU, Fornés A, Galecki A, Miller RA, Burke DT. Multiple-trait quantitative trait loci analysis using a large mouse sibship. Genetics. 1999;151(2):785–795. 23

[40] C Stern1 M, Benavides F, A Klingelberger E, J Conti2 C. Allelotype analysis of chemically induced squamous cell carcinomas in F1 hybrids of two inbred mouse strains with different susceptibility to tumor progression. Carcinogenesis. 2000;21(7):1297–1301. 23

[41] Lasko D, Cavenee W, Nordenskjöld M. Loss of constitutional heterozygosity in human cancer. Annual review of genetics. 1991;25(1):281–314. 23

[42] Allen N, Sudlow C, Downey P, Peakman T, Danesh J, Elliott P, et al. UK Biobank: Current status and what it means for epidemiology. Health Policy and Technology. 2012;1(3):123–126. 26

[43] Spain SL, Barrett JC. Strategies for fine-mapping complex traits. Human molecular genetics. 2015;24(R1):R111–R119. 26

[44] Pirinen M, Donnelly P, Spencer CC, et al. Efficient computation with a linear mixed model on large-scale data sets with applications to genetic studies. The Annals of Applied Statistics. 2013;7(1):369–390. 27, 28

[45] Tseng P, Yun S. A coordinate gradient descent method for nonsmooth separable minimization. Mathematical Programming. 2009;117(1):387–423. 31, 47, 50

[46] Meier L, Van De Geer S, Bühlmann P. The group lasso for logistic regression. Journal of the Royal Statistical Society: Series B (Statistical Methodology). 2008;70(1):53–71. 31, 47

[47] Schelldorfer J, Bühlmann P, DE G, VAN S. Estimation for High-Dimensional Linear Mixed-Effects Models Using L1-Penalization. Scandinavian Journal of Statistics. 2011;38(2):197–214. 31, 39, 47

[48] Byrd RH, Lu P, Nocedal J, Zhu C. A limited memory algorithm for bound constrained optimization. SIAM Journal on Scientific Computing. 1995;16(5):1190–1208. 33

[49] Wakefield J. Bayesian and frequentist regression methods. Springer Science & Business Media; 2013. 36

[50] Nishii R. Asymptotic properties of criteria for selection of variables in multiple regression. The Annals of Statistics. 1984;p. 758–765. 39

[51] Zou H, Hastie T, Tibshirani R, et al. On the degrees of freedom of the lasso. The Annals of Statistics. 2007;35(5):2173–2192. 39

[52] Bondell HD, Krishna A, Ghosh SK. Joint Variable Selection for Fixed and Random Effects in Linear Mixed-Effects Models. Biometrics. 2010;66(4):1069–1077. 39

[53] Fan Y, Tang CY. Tuning parameter selection in high dimensional penalized likeli-hood. Journal of the Royal Statistical Society: Series B (Statistical Methodology). 2013;75(3):531–552. 39

[54] Xie Y. Dynamic Documents with R and knitr. vol. 29. CRC Press; 2015. 60

A   Block Coordinate Descent Algorithm

We use a general purpose block coordinate descent algorithm (CGD) [45] to solve (16). At each iteration, the algorithm approximates the negative log-likelihood $f(\cdot)$ in $Q_\lambda(\cdot)$ by a strictly convex quadratic function and then applies block coordinate decent to generate a decent direction followed by an inexact line search along this direction [45]. For continuously differentiable $f(\cdot)$ and convex and block-separable $P(\cdot)$ (i.e. $P(\boldsymbol{\beta}) = \sum_i P_i(\beta_i)$), [45] show that the solution generated by the CGD method is a stationary point of $Q_\lambda(\cdot)$ if the coordinates are updated in a Gauss-Seidel manner i.e. $Q_\lambda(\cdot)$ is minimized with respect to one parameter while holding all others fixed. The CGD algorithm can thus be run in parallel and therefore suited for large p settings. It has been successfully applied in fixed effects models (e.g. [46], [20]) and [47] for mixed models with an ℓ_1 penalty. Following Tseng and Yun [45], the CGD algorithm is given by Algorithm 2.

The Armijo rule is defined as follows [45]:

Choose $\alpha_{init}^{(k)} > 0$ and let $\alpha^{(k)}$ be the largest element of $\left\{\alpha_{init}^k \delta^r\right\}_{r=0,1,2,\dots}$ satisfying

$$Q_\lambda(\Theta_j^{(k)} + \alpha^{(k)} d^{(k)}) \leq Q_\lambda(\Theta_j^{(k)}) + \alpha^{(k)} \varrho \Delta^{(k)} \tag{44}$$

where $0 < \delta < 1$, $0 < \varrho < 1$, $0 \leq \gamma < 1$ and

$$\Delta^{(k)} := \nabla f(\Theta_j^{(k)}) d^{(k)} + \gamma (d^{(k)})^2 H_{jj}^{(k)} + \lambda P(\Theta_j^{(k)} + d^{(k)}) - \lambda P(\Theta^{(k)}) \tag{45}$$

Common choices for the constants are $\delta = 0.1$, $\varrho = 0.001$, $\gamma = 0$, $\alpha_{init}^{(k)} = 1$ for all k [47].

Below we detail the specifics of Algorithm 2 for the ℓ_1 penalty.

Algorithm 2: Coordinate Gradient Descent Algorithm to solve (16)

Set the iteration counter $k \leftarrow 0$ and choose initial values for the parameter vector $\mathbf{\Theta}^{(0)}$;

repeat

  Approximate the Hessian $\nabla^2 f(\mathbf{\Theta}^{(k)})$ by a symmetric matix $H^{(k)}$:

$$H^{(k)} = \text{diag}\left[\min\left\{\max\left\{\left[\nabla^2 f(\mathbf{\Theta}^{(k)})\right]_{jj}, c_{min}\right\} c_{max}\right\}\right]_{j=1,\ldots,p} \tag{40}$$

  for $j = 1, \ldots, p$ **do**

    Solve the descent direction $d^{(k)} := d_{H^{(k)}}(\Theta_j^{(k)})$;

    if $\Theta_j^{(k)} \in \{\beta_1, \ldots, \beta_p\}$ **then**

$$d_{H^{(k)}}(\Theta_j^{(k)}) \leftarrow \arg\min_{d}\left\{\nabla f(\Theta_j^{(k)})d + \frac{1}{2}d^2 H_{jj}^{(k)} + \lambda P(\Theta_j^{(k)} + d)\right\} \tag{41}$$

    end

  end

  Choose a stepsize;

$$\alpha_j^{(k)} \leftarrow \text{line search given by the Armijo rule}$$

  Update;

$$\widehat{\Theta}_j^{(k+1)} \leftarrow \widehat{\Theta}_j^{(k)} + \alpha_j^{(k)} d^{(k)}$$

  Update;

$$\widehat{\eta}^{(k+1)} \leftarrow \arg\min_{\eta} \frac{1}{2}\sum_{i=1}^{N_T}\log(1+\eta(\Lambda_i-1)) + \frac{1}{2\sigma^{2\,(k)}}\sum_{i=1}^{N_T}\frac{\left(\widetilde{Y}_i - \sum_{j=0}^{p}\widetilde{X}_{ij+1}\beta_j^{(k+1)}\right)^2}{1+\eta(\Lambda_i-1)} \tag{42}$$

  Update;

$$\widehat{\sigma^2}^{\,(k+1)} \leftarrow \frac{1}{N_T}\sum_{i=1}^{N_T}\frac{\left(\widetilde{Y}_i - \sum_{j=0}^{p}\widetilde{X}_{ij+1}\beta_j^{(k+1)}\right)^2}{1+\eta^{(k+1)}(\Lambda_i-1)} \tag{43}$$

  $k \leftarrow k + 1$

until *convergence criterion is satisfied*;

A.1 ℓ_1 penalty

The objective function is given by

$$Q_\lambda(\boldsymbol{\Theta}) = f(\boldsymbol{\Theta}) + \lambda|\boldsymbol{\beta}| \tag{46}$$

A.1.1   Descent Direction

For simplicity, we remove the iteration counter (k) from the derivation below.

For $\Theta_j^{(k)} \in \{\beta_1, \dots, \beta_p\}$, let

$$d_H(\Theta_j) = \arg\min_d G(d) \tag{47}$$

where

$$G(d) = \nabla f(\Theta_j)d + \frac{1}{2}d^2 H_{jj} + \lambda|\Theta_j + d|$$

Since $G(d)$ is not differentiable at $-\Theta_j$, we calculate the subdifferential $\partial G(d)$ and search for d with $0 \in \partial G(d)$:

$$\partial G(d) = \nabla f(\Theta_j) + dH_{jj} + \lambda u \tag{48}$$

where

$$u = \begin{cases} 1 & \text{if} \quad d > -\Theta_j \\ -1 & \text{if} \quad d < -\Theta_j \\ [-1, 1] & \text{if} \quad d = \Theta_j \end{cases} \tag{49}$$

We consider each of the three cases in (48) below

1. $d > -\Theta_j$

$$\partial G(d) = \nabla f(\Theta_j) + dH_{jj} + \lambda = 0$$
$$d = \frac{-(\nabla f(\Theta_j) + \lambda)}{H_{jj}}$$

Since $\lambda > 0$ and $H_{jj} > 0$, we have

$$\frac{-(\nabla f(\Theta_j) - \lambda)}{H_{jj}} > \frac{-(\nabla f(\Theta_j) + \lambda)}{H_{jj}} = d \overset{\text{def}}{>} -\Theta_j$$

The solution can be written compactly as

$$d = \text{mid} \left\{ \frac{-(\nabla f(\Theta_j) - \lambda)}{H_{jj}}, -\Theta_j, \frac{-(\nabla f(\Theta_j) + \lambda)}{H_{jj}} \right\}$$

where $\text{mid}\{a, b, c\}$ denotes the median (mid-point) of a, b, c [45].

2. $d < -\Theta_j$

$$\partial G(d) = \nabla f(\Theta_j) + dH_{jj} - \lambda = 0$$
$$d = \frac{-(\nabla f(\Theta_j) - \lambda)}{H_{jj}}$$

Since $\lambda > 0$ and $H_{jj} > 0$, we have

$$\frac{-(\nabla f(\Theta_j) + \lambda)}{H_{jj}} < \frac{-(\nabla f(\Theta_j) - \lambda)}{H_{jj}} = d \overset{\text{def}}{<} -\Theta_j$$

Again, the solution can be written compactly as

$$d = \text{mid} \left\{ \frac{-(\nabla f(\Theta_j) - \lambda)}{H_{jj}}, -\Theta_j, \frac{-(\nabla f(\Theta_j) + \lambda)}{H_{jj}} \right\}$$

3. $d_j = -\Theta_j$

There exists $u \in [-1, 1]$ such that

$$\partial G(d) = \nabla f(\Theta_j) + dH_{jj} + \lambda u = 0$$
$$d = \frac{-(\nabla f(\Theta_j) + \lambda u)}{H_{jj}}$$

For $-1 \leq u \leq 1$, $\lambda > 0$ and $H_{jj} > 0$ we have

$$\frac{-(\nabla f(\Theta_j) + \lambda)}{H_{jj}} \leq d \stackrel{\text{def}}{=} -\Theta_j \leq \frac{-(\nabla f(\Theta_j) - \lambda)}{H_{jj}}$$

The solution can again be written compactly as

$$d = \text{mid} \left\{ \frac{-(\nabla f(\Theta_j) - \lambda)}{H_{jj}}, -\Theta_j, \frac{-(\nabla f(\Theta_j) + \lambda)}{H_{jj}} \right\}$$

We see all three cases lead to the same solution for (47). Therefore the descent direction for $\Theta_j^{(k)} \in \{\beta_1, \ldots, \beta_p\}$ for the ℓ_1 penalty is given by

$$d = \text{mid} \left\{ \frac{-(\nabla f(\beta_j) - \lambda)}{H_{jj}}, -\beta_j, \frac{-(\nabla f(\beta_j) + \lambda)}{H_{jj}} \right\} \tag{50}$$

A.1.2   Solution for the β parameter

If the Hessian $\nabla^2 f(\boldsymbol{\Theta}^{(k)}) > 0$ then $H^{(k)}$ defined in (40) is equal to $\nabla^2 f(\boldsymbol{\Theta}^{(k)})$. Using $\alpha_{init} = 1$, the largest element of $\left\{ \alpha_{init}^{(k)} \delta^r \right\}_{r=0,1,2,\ldots}$ satisfying the Armijo Rule inequality is reached for $\alpha^{(k)} = \alpha_{init}^{(k)} \delta^0 = 1$. The Armijo rule update for the $\boldsymbol{\beta}$ parameter is then given by

$$\beta_j^{(k+1)} \leftarrow \beta_j^{(k)} + d^{(k)}, \qquad j = 1, \ldots, p \tag{51}$$

Substituting the descent direction given by (50) into (51) we get

$$\beta_j^{(k+1)} = \text{mid} \left\{ \beta_j^{(k)} + \frac{-(\nabla f(\beta_j^{(k)}) - \lambda)}{H_{jj}}, 0, \beta_j^{(k)} + \frac{-(\nabla f(\beta_j^{(k)}) + \lambda)}{H_{jj}} \right\} \tag{52}$$

We can further simplify this expression. Let

$$w_i := \frac{1}{\sigma^2 \left(1 + \eta(\Lambda_i - 1)\right)} \tag{53}$$

610   .

Re-write the part depending on $\boldsymbol{\beta}$ of the negative log-likelihood in (14) as

$$g(\boldsymbol{\beta}^{(k)}) = \frac{1}{2} \sum_{i=1}^{N_T} w_i \left(\widetilde{Y}_i - \sum_{\ell \neq j} \widetilde{X}_{i\ell} \beta_\ell^{(k)} - \widetilde{X}_{ij} \beta_j^{(k)} \right)^2 \tag{54}$$

The gradient and Hessian are given by

$$\nabla f(\beta_j^{(k)}) := \frac{\partial}{\partial \beta_j^{(k)}} g(\boldsymbol{\beta}^{(k)}) = -\sum_{i=1}^{N_T} w_i \widetilde{X}_{ij} \left(\widetilde{Y}_i - \sum_{\ell \neq j} \widetilde{X}_{i\ell} \beta_\ell^{(k)} - \widetilde{X}_{ij} \beta_j^{(k)} \right) \tag{55}$$

$$H_{jj} := \frac{\partial^2}{\partial \beta_j^{(k)2}} g(\boldsymbol{\beta}^{(k)}) = \sum_{i=1}^{N_T} w_i \widetilde{X}_{ij}^2 \tag{56}$$

Substituting (55) and (56) into $\beta_j^{(k)} + \frac{-(\nabla f(\beta_j^{(k)}) - \lambda)}{H_{jj}}$

$$\begin{aligned}
\beta_j^{(k)} &+ \frac{\sum_{i=1}^{N_T} w_i \widetilde{X}_{ij} \left(\widetilde{Y}_i - \sum_{\ell \neq j} \widetilde{X}_{i\ell} \beta_\ell^{(k)} - \widetilde{X}_{ij} \beta_j^{(k)} \right) + \lambda}{\sum_{i=1}^{N_T} w_i \widetilde{X}_{ij}^2} \\
&= \beta_j^{(k)} + \frac{\sum_{i=1}^{N_T} w_i \widetilde{X}_{ij} \left(\widetilde{Y}_i - \sum_{\ell \neq j} \widetilde{X}_{i\ell} \beta_\ell^{(k)} \right) + \lambda}{\sum_{i=1}^{N_T} w_i \widetilde{X}_{ij}^2} - \frac{\sum_{i=1}^{N_T} w_i \widetilde{X}_{ij}^2 \beta_j^{(k)}}{\sum_{i=1}^{N_T} w_i \widetilde{X}_{ij}^2} \\
&= \frac{\sum_{i=1}^{N_T} w_i \widetilde{X}_{ij} \left(\widetilde{Y}_i - \sum_{\ell \neq j} \widetilde{X}_{i\ell} \beta_\ell^{(k)} \right) + \lambda}{\sum_{i=1}^{N_T} w_i \widetilde{X}_{ij}^2}
\end{aligned} \tag{57}$$

Similarly, substituting (55) and (56) in $\beta_j^{(k)} + \frac{-(\nabla f(\beta_j^{(k)}) + \lambda)}{H_{jj}}$ we get

$$\frac{\sum_{i=1}^{N_T} w_i \widetilde{X}_{ij} \left(\widetilde{Y}_i - \sum_{\ell \neq j} \widetilde{X}_{i\ell} \beta_\ell^{(k)} \right) - \lambda}{\sum_{i=1}^{N_T} w_i \widetilde{X}_{ij}^2} \tag{58}$$

Finally, substituting (57) and (58) into (52) we get

$$\beta_j^{(k+1)} = \text{mid} \left\{ \frac{\sum_{i=1}^{N_T} w_i \widetilde{X}_{ij} \left(\widetilde{Y}_i - \sum_{\ell \neq j} \widetilde{X}_{i\ell} \beta_\ell^{(k)} \right) - \lambda}{\sum_{i=1}^{N_T} w_i \widetilde{X}_{ij}^2}, 0, \frac{\sum_{i=1}^{N_T} w_i \widetilde{X}_{ij} \left(\widetilde{Y}_i - \sum_{\ell \neq j} \widetilde{X}_{i\ell} \beta_\ell^{(k)} \right) + \lambda}{\sum_{i=1}^{N_T} w_i \widetilde{X}_{ij}^2} \right\}$$

$$= \frac{\mathcal{S}_\lambda \left(\sum_{i=1}^{N_T} w_i \widetilde{X}_{ij} \left(\widetilde{Y}_i - \sum_{\ell \neq j} \widetilde{X}_{i\ell} \beta_\ell^{(k)} \right) \right)}{\sum_{i=1}^{N_T} w_i \widetilde{X}_{ij}^2} \tag{59}$$

Where $\mathcal{S}_\lambda(x)$ is the soft-thresholding operator

$$\mathcal{S}_\lambda(x) = \text{sign}(x)(|x| - \lambda)_+$$

$\text{sign}(x)$ is the signum function

$$\text{sign}(x) = \begin{cases} -1 & x < 0 \\ 0 & x = 0 \\ 1 & x > 0 \end{cases}$$

611   and $(x)_+ = \max(x, 0)$.

B   Additional Simulation Results
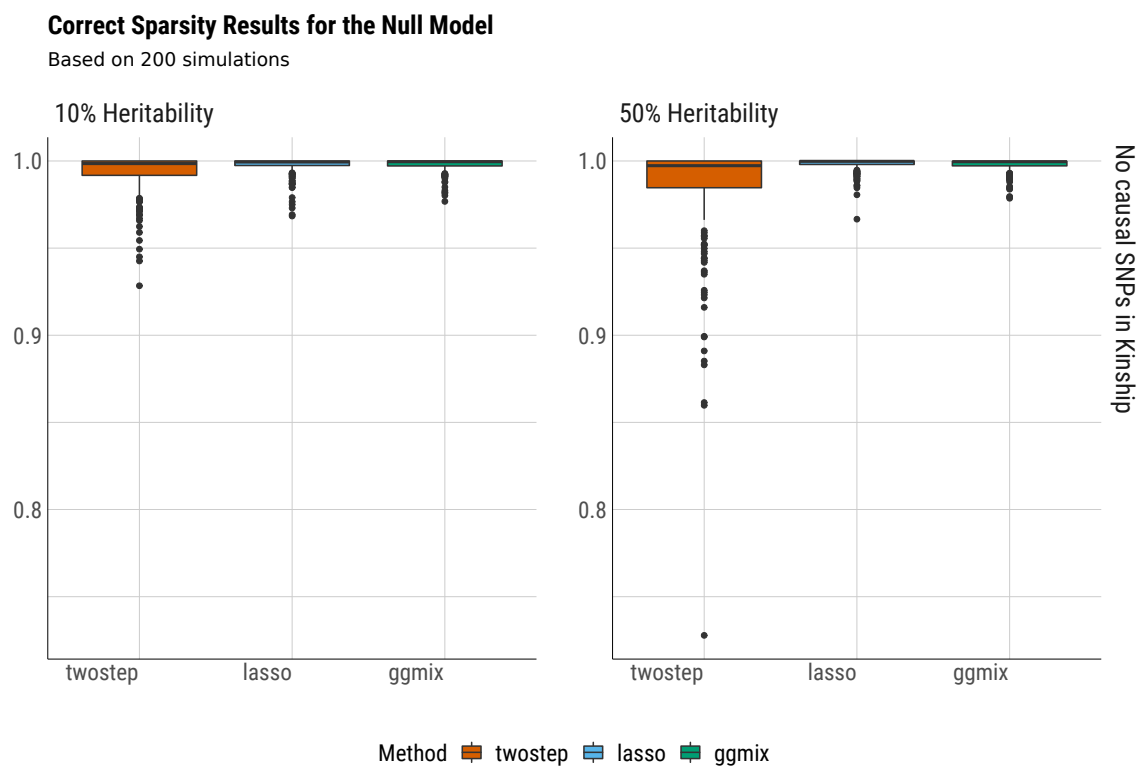
Figure 15: Boxplots of the correct sparsity from 200 simulations by the true heritability $\eta = \{10\%, 50\%\}$ for the null model ($c = 0$).
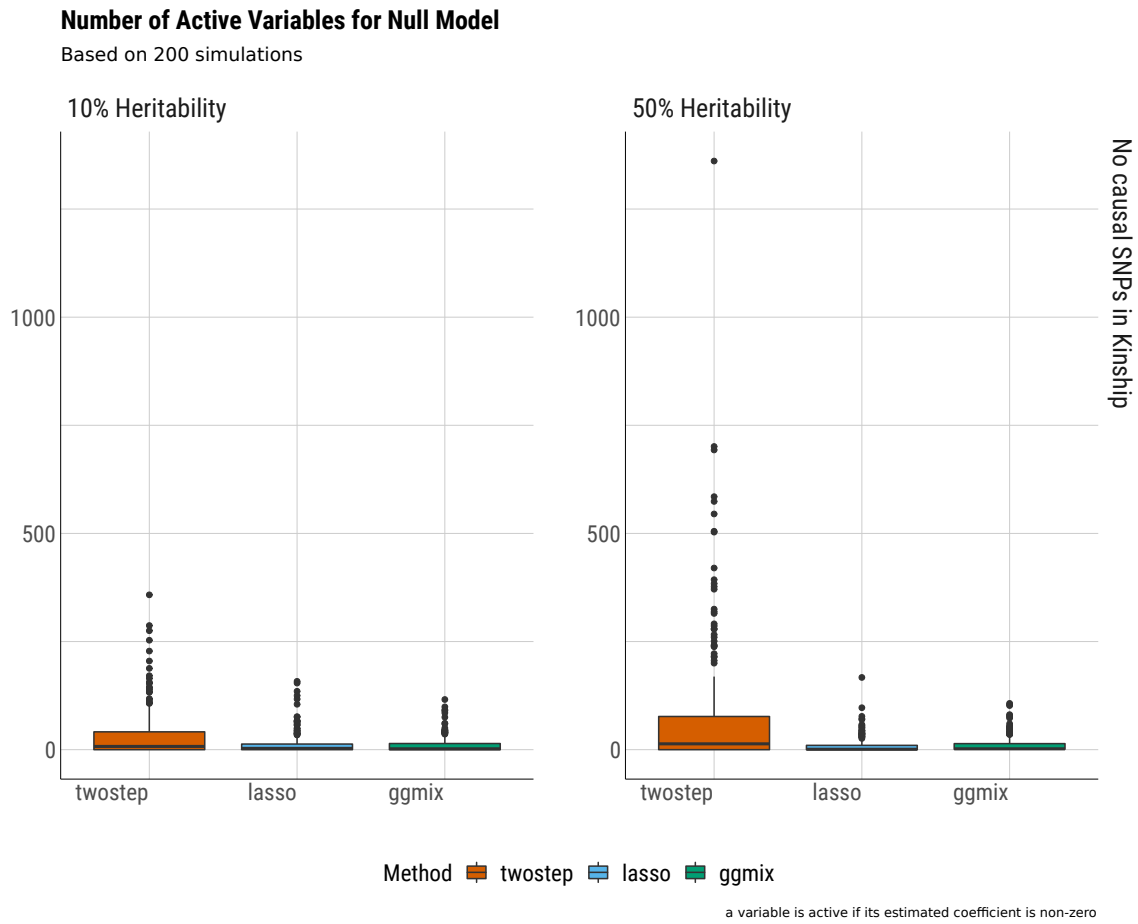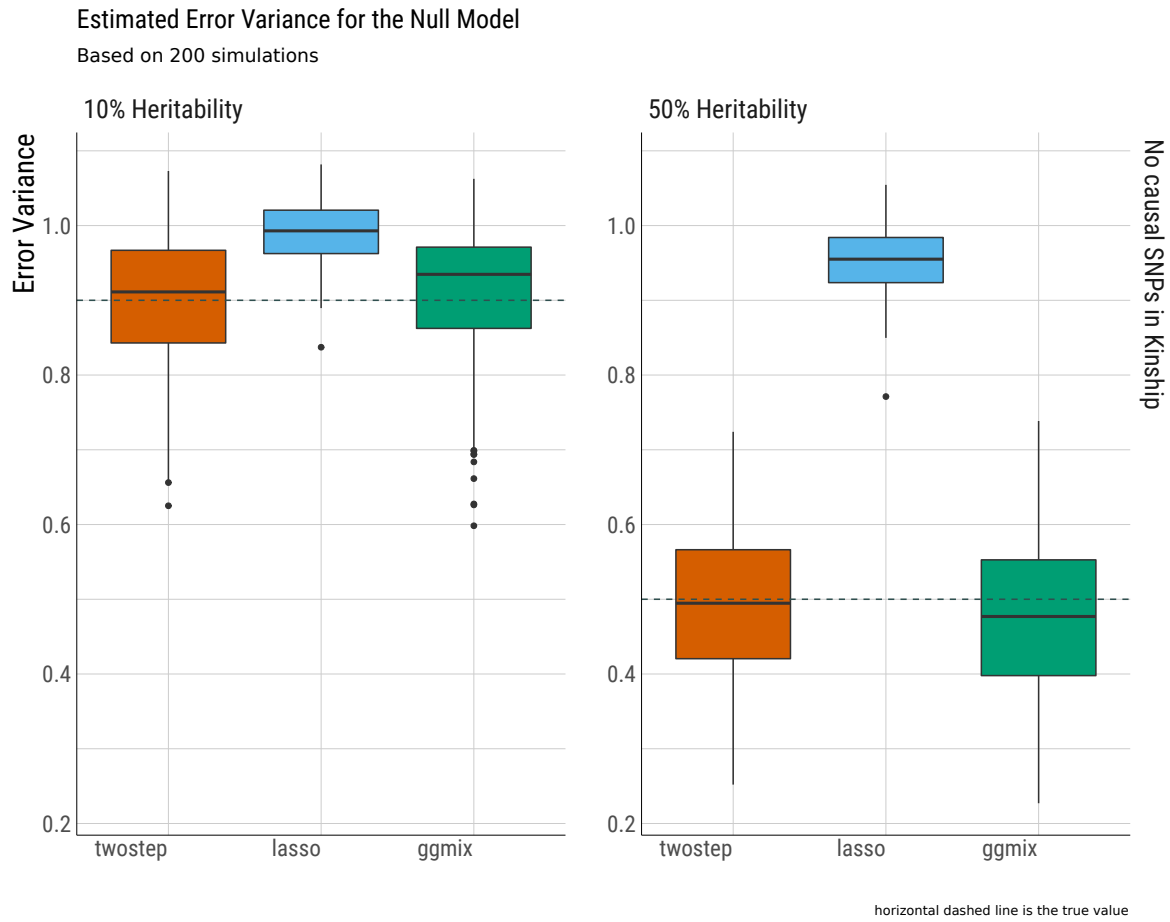
Figure 16: Boxplots of the number of active variables from 200 simulations by the true heritability $\eta = \{10\%, 50\%\}$ for the null model ($c = 0$).
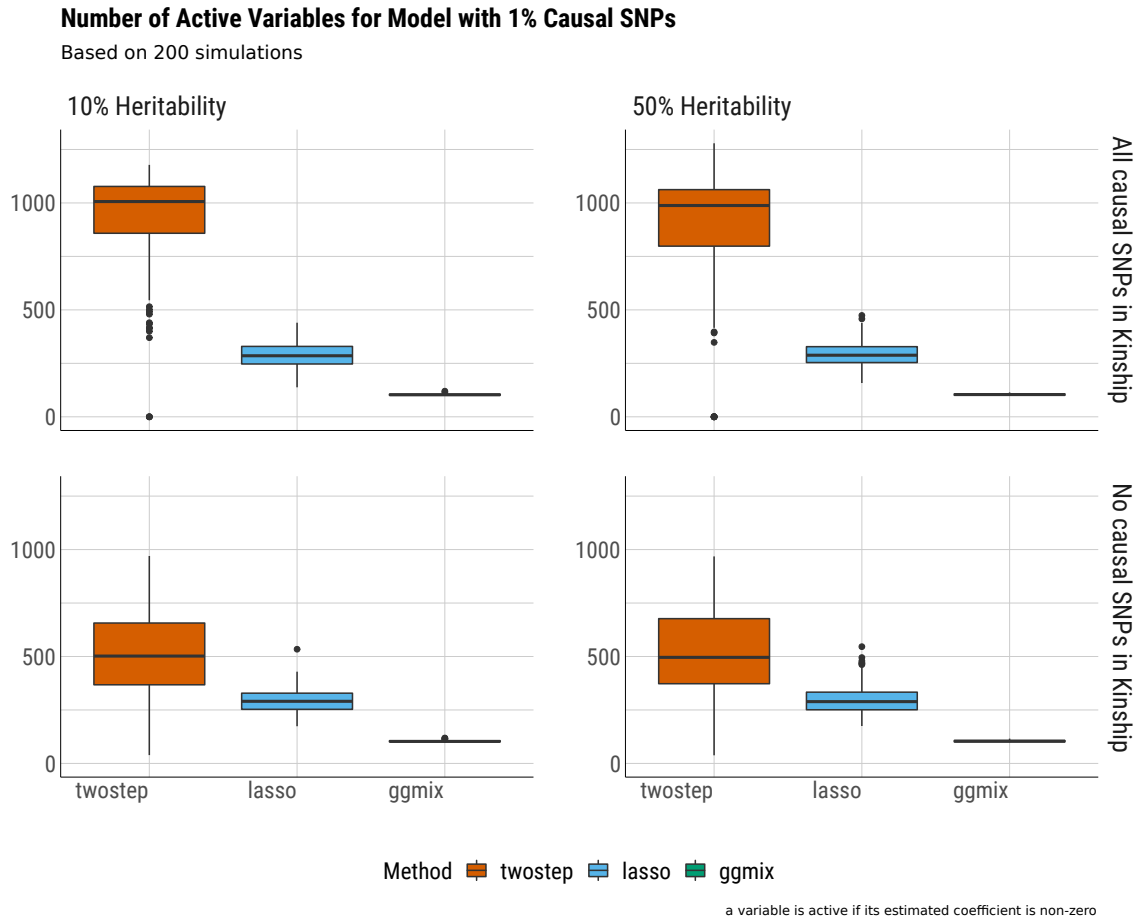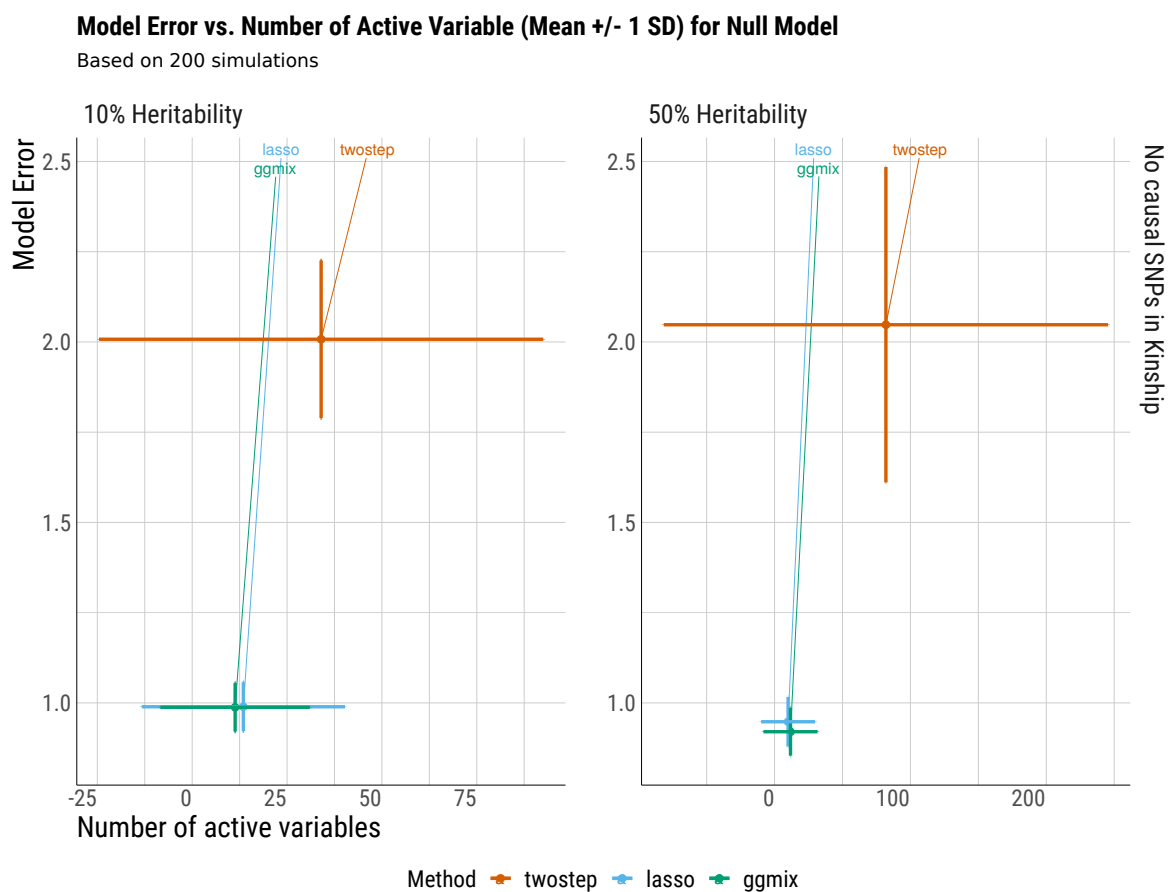
Figure 17: Boxplots of the number of active variables from 200 simulations by the true heritability $\eta = \{10\%, 50\%\}$ and number of causal SNPs that were included in the calculation of the kinship matrix for the model with 1% causal SNPs ($c = 0.01$).
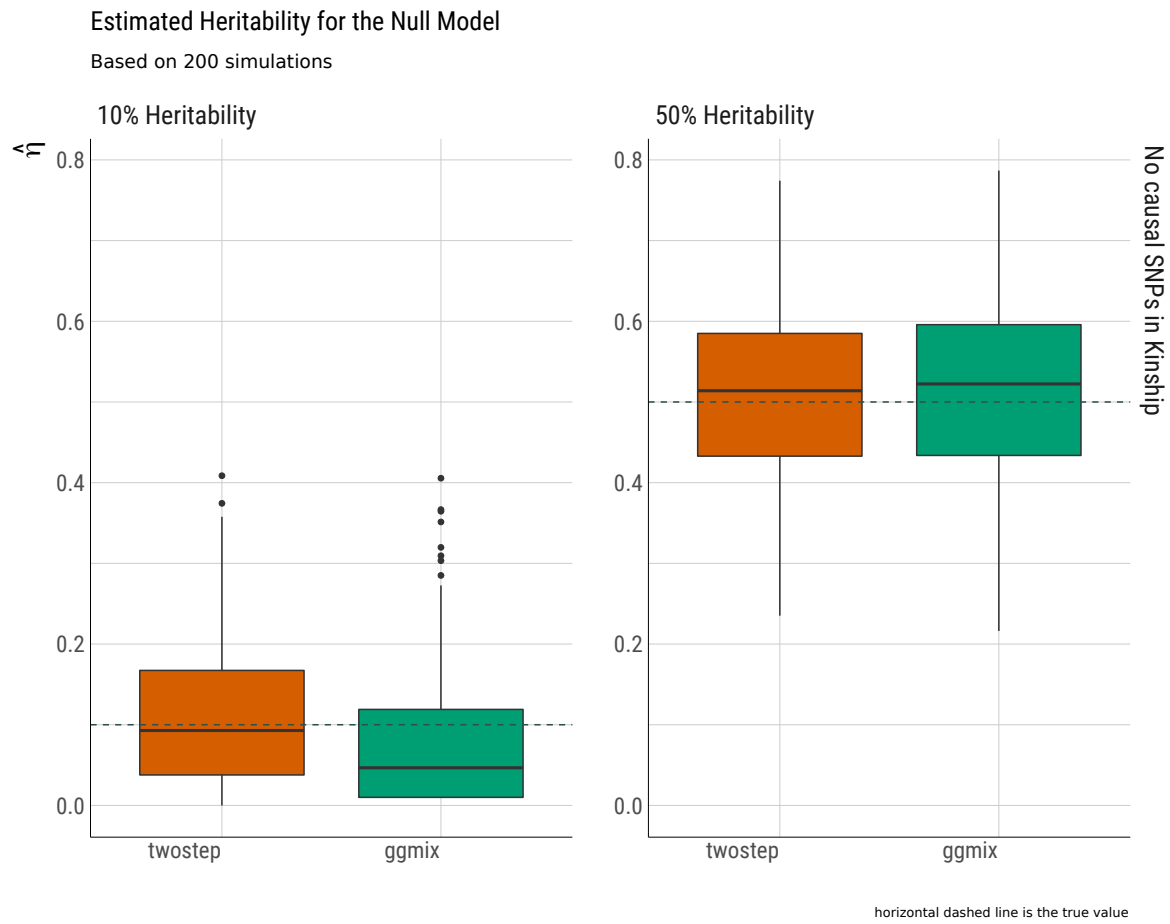
Figure 18: Boxplots of the heritability estimate $\hat{\eta}$ from 200 simulations by the true heritability $\eta = \{10\%, 50\%\}$ for the null model ($c = 0$).

Figure 19: Boxplots of the estimated error variance from 200 simulations by the true heritability $\eta = \{10\%, 50\%\}$ for the null model ($c = 0$).

Figure 20: Means ±1 standard deviation of the model error vs. the number of active variables by the true heritability $\eta = \{10\%, 50\%\}$ for the null model ($c = 0$).

C   `ggmix` Package Showcase

In this section we briefly introduce the freely available and open source `ggmix` package in `R`. More comprehensive documentation is available at https://sahirbhatnagar.com/ggmix. Note that this entire section is reproducible; the code and text are combined in an `.Rnw`[1] file and compiled using `knitr` [54].

C.1   Installation

The package can be installed from GitHub via

```
install.packages("pacman")
pacman::p_load_gh('sahirbhatnagar/ggmix')
```

To showcase the main functions in `ggmix`, we will use the simulated data which ships with the package and can be loaded via:

```
library(ggmix)
data("admixed")
names(admixed)

##  [1] "y"              "x"               "causal"
##  [4] "beta"           "kin"             "Xkinship"
##  [7] "not_causal"     "causal_positive" "causal_negative"
## [10] "x_lasso"
```

For details on how this data was simulated, see `help(admixed)`.

There are three basic inputs that `ggmix` needs:

1. Y: a continuous response variable

2. X: a matrix of covariates of dimension $N \times p$ where N is the sample size and p is the number of covariates

3. $\mathbf{\Phi}$: a kinship matrix

---

[1]scripts available at https://github.com/sahirbhatnagar/ggmix/tree/master/manuscript

₆₂₈ We can visualize the kinship matrix in the `admixed` data using the `popkin` package:

```
# need to install the package if you don't have it
# pacman::p_load_gh('StoreyLab/popkin')
popkin::plotPopkin(admixed$kin)
```

₆₂₉
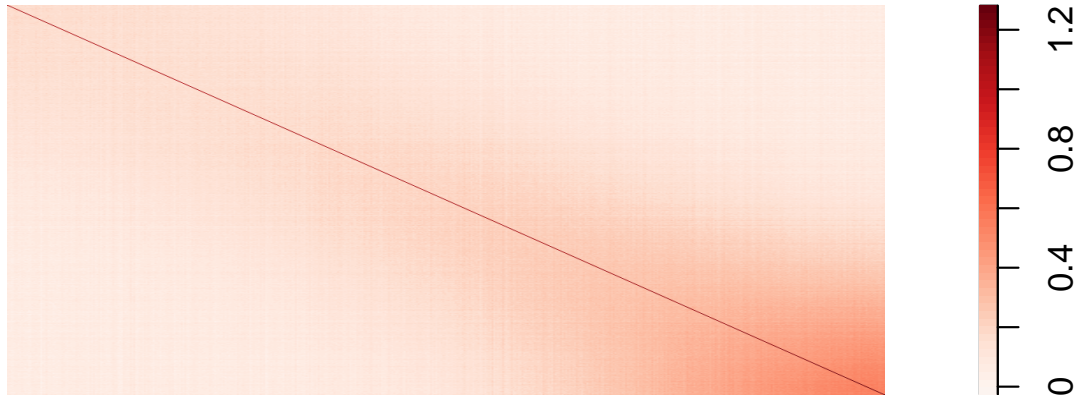
C.2 Fit the linear mixed model with Lasso Penalty

₆₃₁ We will use the most basic call to the main function of this package, which is called `ggmix`.

₆₃₂ This function will by default fit a L_1 penalized linear mixed model (LMM) for 100 distinct

₆₃₃ values of the tuning parameter λ. It will choose its own sequence:

```
fit <- ggmix(x = admixed$x, y = admixed$y, kinship = admixed$kin)
```

```
names(fit)

## [1] "result"       "ggmix_object" "n_design"      "p_design"
## [5] "lambda"       "coef"         "b0"            "beta"
## [9] "df"           "eta"          "sigma2"        "nlambda"
## [13] "cov_names"    "call"

class(fit)

## [1] "lassofullrank" "ggmix_fit"
```
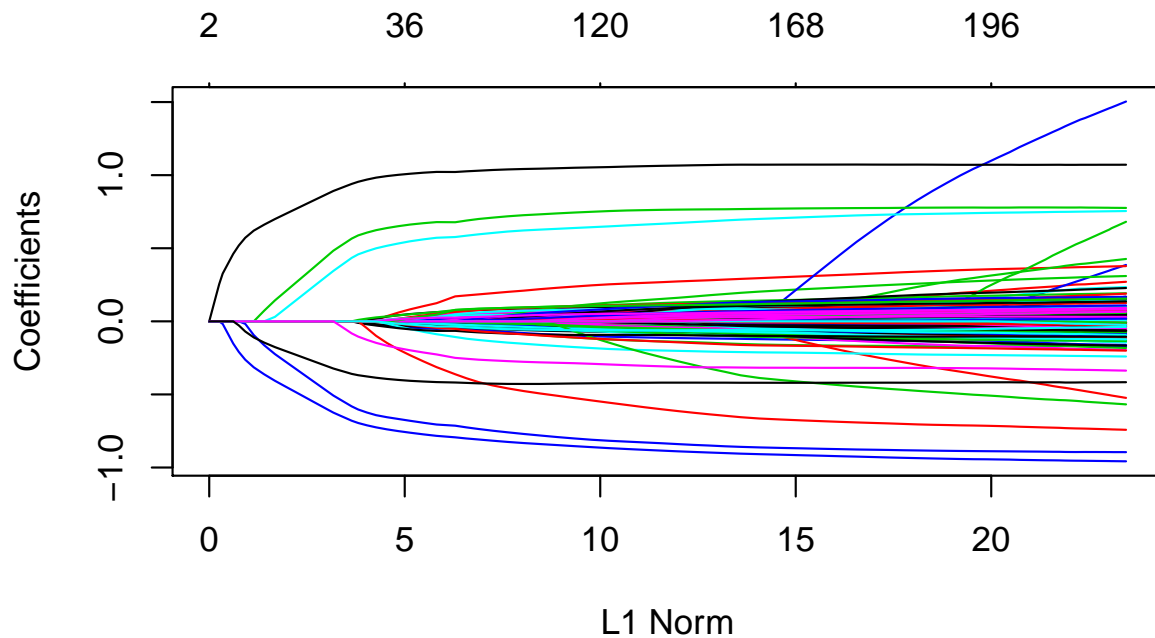
634 We can see the solution path for each variable by calling the `plot` method for objects of

635 class `ggmix_fit`:

```
plot(fit)
```


636

637 We can also get the coefficients for given value(s) of lambda using the `coef` method for

638 objects of class `ggmix_fit`:

```
# only the first 5 coefficients printed here for brevity
```

```
coef(fit, s = c(0.1,0.02))[1:5, ]

## 5 x 2 Matrix of class "dgeMatrix"
##                        1           2
## (Intercept) -0.3824525 -0.030224599
## X62          0.0000000  0.000000000
## X185         0.0000000  0.001444518
## X371         0.0000000  0.009513475
## X420         0.0000000  0.000000000
```

₆₃₉ Here, `s` specifies the value(s) of λ at which the extraction is made. The function uses linear

₆₄₀ interpolation to make predictions for values of `s` that do not coincide with the lambda

₆₄₁ sequence used in the fitting algorithm.

₆₄₂ We can also get predictions $(X\widehat{\boldsymbol{\beta}})$ using the `predict` method for objects of class `ggmix_fit`:

```
# need to provide x to the predict function
# predict for the first 5 subjects
predict(fit, s = c(0.1,0.02), newx = admixed$x[1:5,])

##                   1          2
## id1 -1.19165061 -1.3123392
## id2 -0.02913052  0.3885923
## id3 -2.00084875 -2.6460043
## id4 -0.37255277 -0.9542463
## id5 -1.03967831 -2.1377268
```

₆₄₃ C.3 Find the Optimal Value of the Tuning Parameter

₆₄₄ We use the Generalized Information Criterion (GIC) to select the optimal value for λ. The

₆₄₅ default is $a_n = log(log(n)) * log(p)$ which corresponds to a high-dimensional BIC (HD-

₆₄₆ BIC):

```
# pass the fitted object from ggmix to the gic function:
```

```
hdbic <- gic(fit)

class(hdbic)

## [1] "ggmix_gic"    "lassofullrank" "ggmix_fit"

# we can also fit the BIC by specifying the an argument

bicfit <- gic(fit, an = log(length(admixed$y)))
```
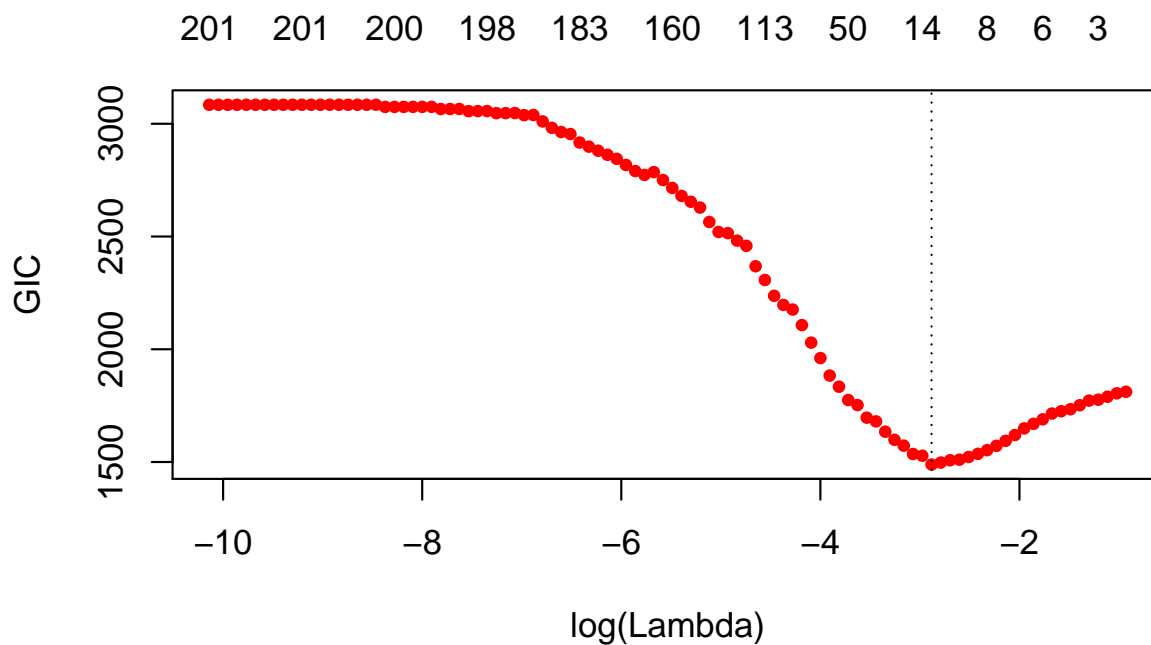
We can plot the HDBIC values against $\log(\lambda)$ using the `plot` method for objects of class `ggmix_gic`:

```
plot(hdbic)
```


The optimal value for λ according to the HDBIC, i.e., the λ that leads to the minium HDBIC is:
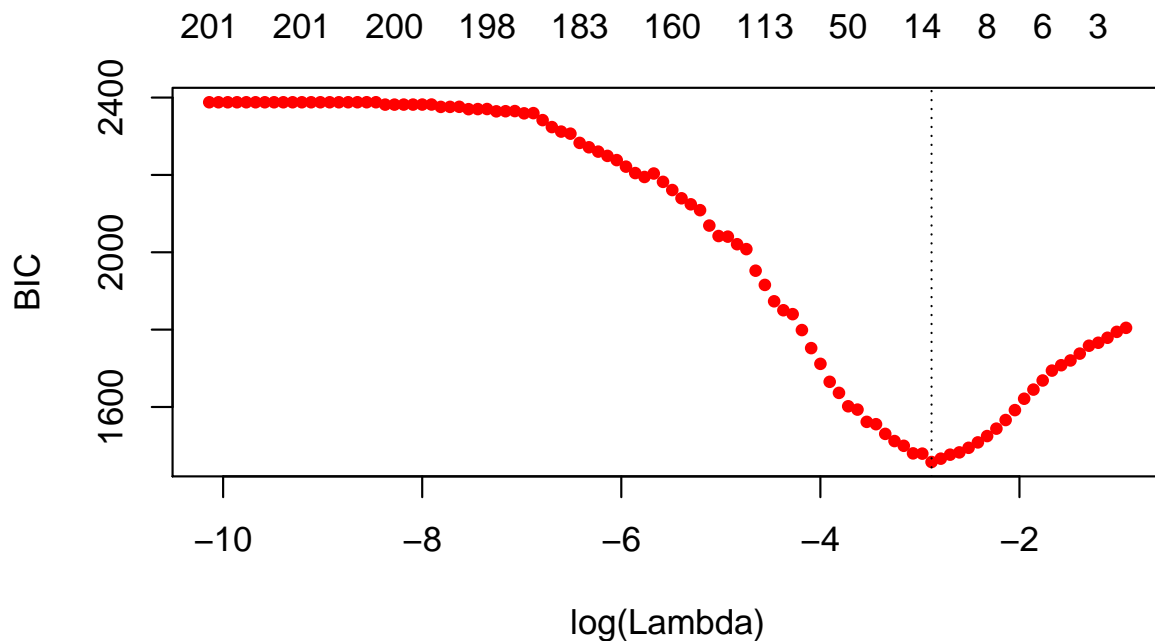
```
hdbic[["lambda.min"]]

## [1] 0.05596623
```

We can also plot the BIC results:

```
plot(bicfit, ylab = "BIC")
```

```
bicfit[["lambda.min"]]

## [1] 0.05596623
```

C.4 Get Coefficients Corresponding to Optimal Model

We can use the object outputted by the `gic` function to extract the coefficients corresponding to the selected model using the `coef` method for objects of class `ggmix_gic`:

```
coef(hdbic)[1:5, , drop = FALSE]

## 5 x 1 sparse Matrix of class "dgCMatrix"
##                     1
## (Intercept) -0.2668419
## X62           .
## X185          .
## X371          .
## X420          .
```

We can also extract just the nonzero coefficients which also provide the estimated variance

658 components η and σ^2:

```
coef(hdbic, type = "nonzero")

##                      1
## (Intercept) -0.26684191
## X336         -0.67986393
## X7638         0.43403365
## X1536         0.93994982
## X1943         0.56600730
## X2849        -0.58157979
## X56          -0.08244685
## X4106        -0.35939830
## eta           0.26746240
## sigma2        0.98694300
```

659 We can also make predictions from the `hdbic` object, which by default will use the model

660 corresponding to the optimal tuning parameter:

```
predict(hdbic, newx = admixed$x[1:5,])

##              1
## id1 -1.3061041
## id2  0.2991654
## id3 -2.3453664
## id4 -0.4486012
## id5 -1.3895793
```

C.5   Extracting Random Effects

662 The user can compute the random effects using the provided `ranef` method for objects of

663 class `ggmix_gic`. This command will compute the estimated random effects for each subject

664 using the parameters of the selected model:

```
ranef(hdbic)[1:5]

## [1] -0.02548691 -0.10011680  0.13020240 -0.30650997  0.16045768
```

C.6   Diagnostic Plots

We can also plot some standard diagnotic plots such as the observed vs. predicted response, QQ-plots of the residuals and random effects and the Tukey-Anscombe plot. These can be plotted using the `plot` method on a `ggmix_gic` object as shown below.

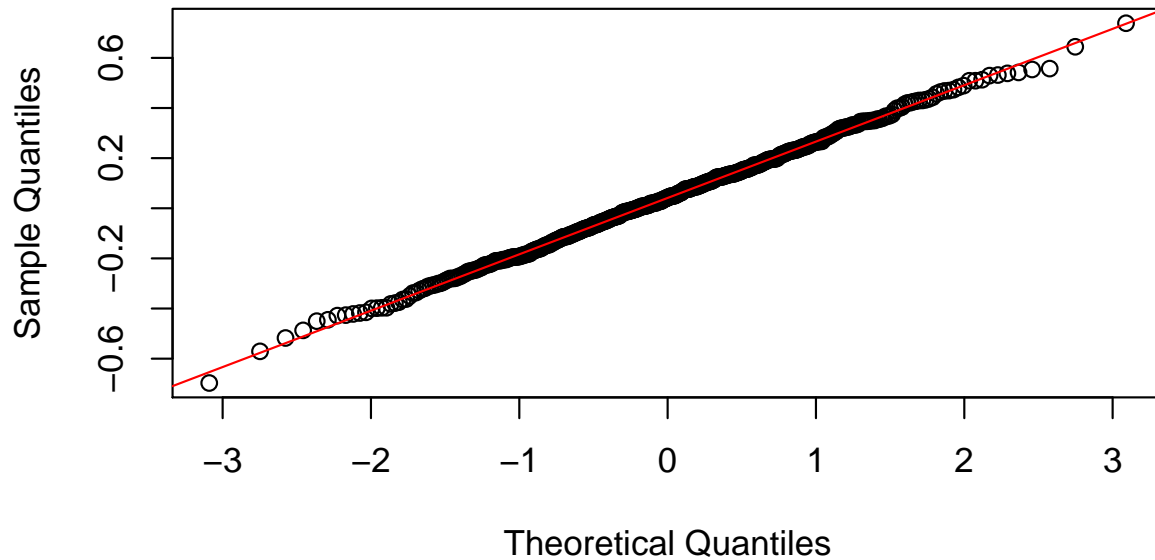### C.6.1   Observed vs. Predicted Response

```
plot(hdbic, type = "predicted", newx = admixed$x, newy = admixed$y)
```


Observed vs. Predicted response

corr(observed,predicted)^2 = 0.77066
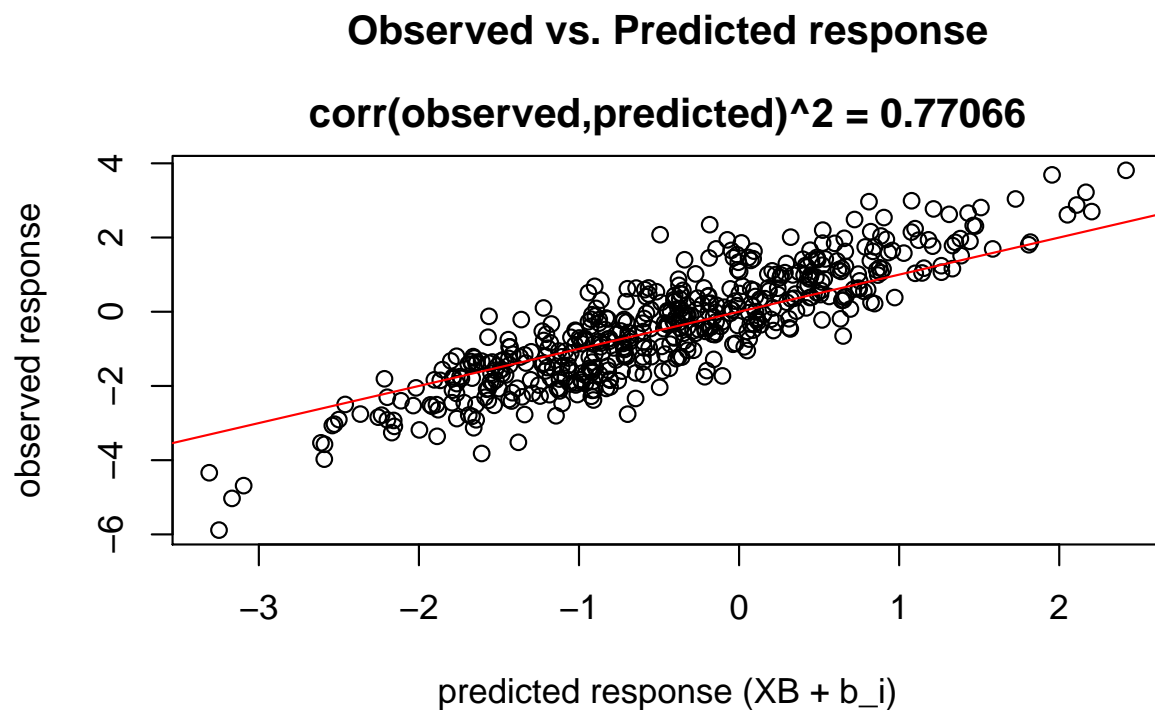
C.6.2   QQ-plots for Residuals and Random Effects

```
plot(hdbic, type = "QQranef", newx = admixed$x, newy = admixed$y)
```
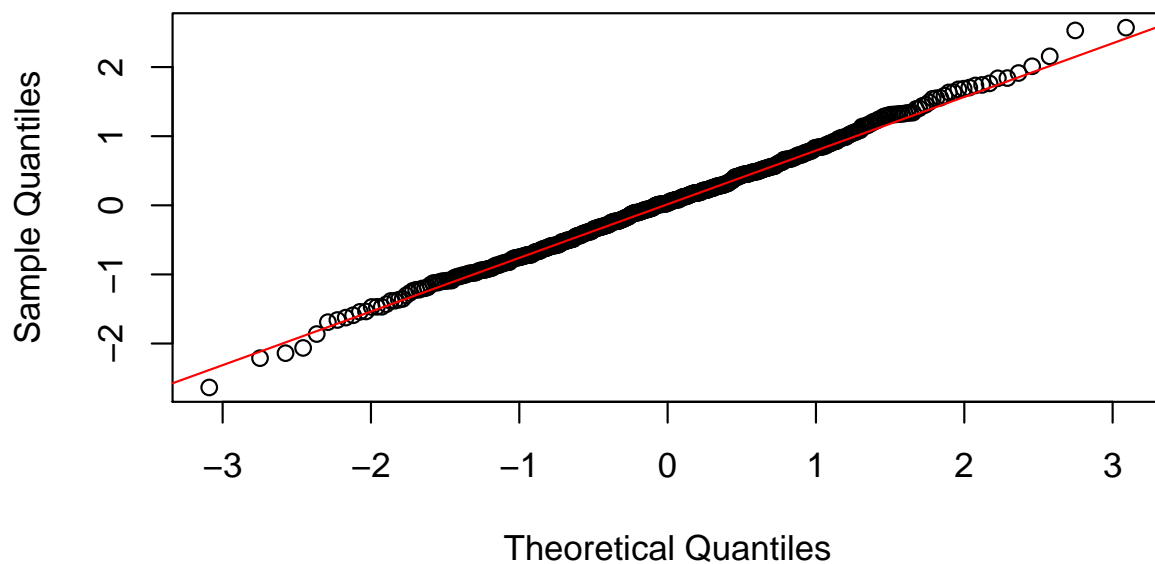
QQ–Plot of the random effects at lambda = 0.06

672

```
plot(hdbic, type = "QQresid", newx = admixed$x, newy = admixed$y)
```
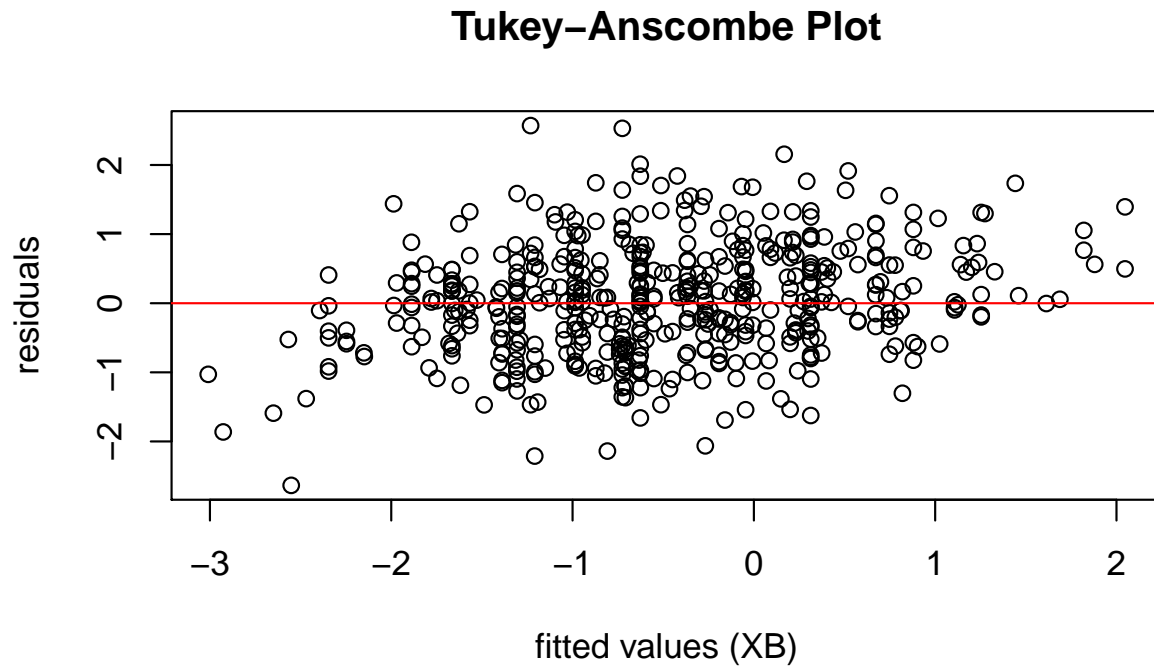
QQ–Plot of the residuals at lambda = 0.06

673

674 **C.6.3   Tukey-Anscombe Plot**

```
plot(hdbic, type = "Tukey", newx = admixed$x, newy = admixed$y)
```

Tukey–Anscombe Plot

675